$\Lambda^*(1520)$ Photoproduction off *Proton* and *Neutron*

from CLAS eg3 data set

Zhiwen Zhao

NSTAR 2011

2011/05/19

- Physics motivation
- Data analysis
- Results
- Summary

Physics Motivation

Λ(1520) **I(J ^{P}) = 0(3/2 $^{-}$)**

Mass m = 1519.5 ± 1.0 MeV **Full width Γ = 15.6 ± 1.0 MeV**

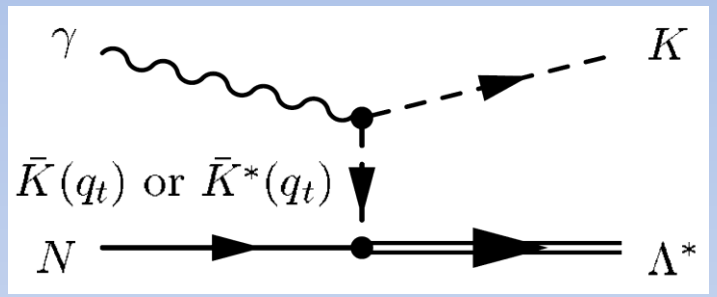

- Its production mechanism is poorly understood due to lack of data.
- Existing data suggest dominance of t-channel processes and K, K* exchange.
- Several model predictions for total and differential cross sections are available.
- Measurement of cross section and decay angular distribution can provide constraints on model prediction and insights into the production mechanism.
- Possible missing N* resonances may decay through strange channels.

Published Experiment

1. on *Proton*

photoproduction measurements

[1] A. Boyarski *et al*.,	(LAMP2, Daresbury),	(1971)
[2] D. Barber *et al.*,	(SLAC),	(1980)
[3] N. Muramatsu *et al.,*	(LEPS),	(2009)
[4] H. Kohri et al.,	(LEPS),	(2010)
[5] F. W. Wieland et al.,	(SAPHIR),	(2010)

electroproduction measurements

[5] T. Azemoon *et al*.,	(DESY),	(1975)
[6] S. P. Barrow *et al.*	(CLAS, JLab),	(2001)
[7] Y. Qiang et al.	(Hall-A, JLab),	(2010)

2. on *Neutron*

photoproduction measurements

[3] N. Muramatsu *et al.,*	(LEPS),	(2009)

Published Theory

S. Nam et al. Phys. Rev. D, 71, 114012 (2005)
S. Nam et al. Phys. Rev. D, 75, 014027 (2007)
S. Nam et al. Phys. Rev. C, 81, 055206 (2010)
A. Titov et al. Phys. Rev. C, 72, 035206 (2005)

Cross Section photoproduction

Comparing *Proton* results between data and theory

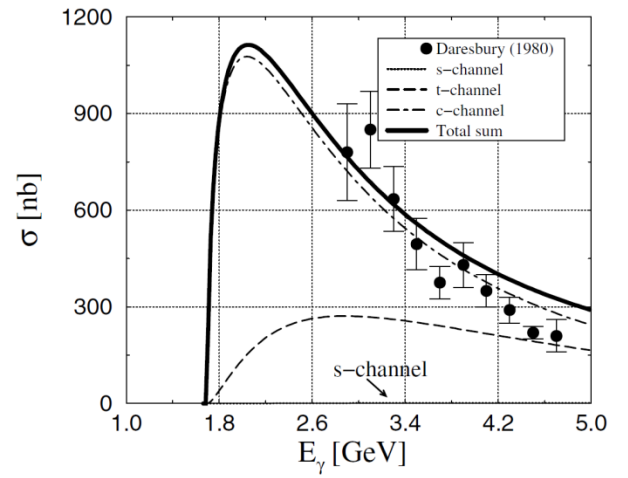

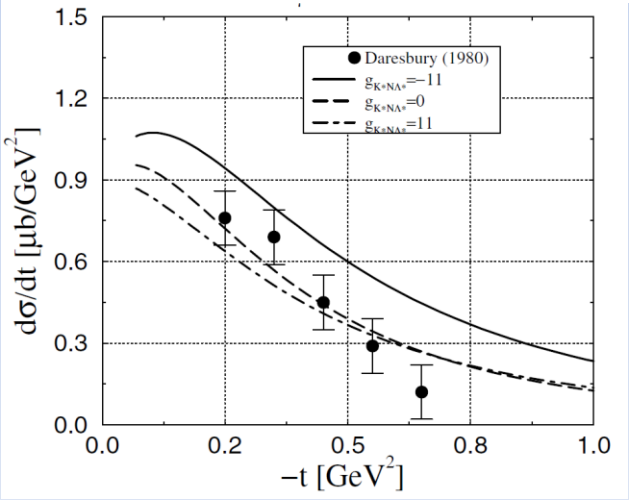

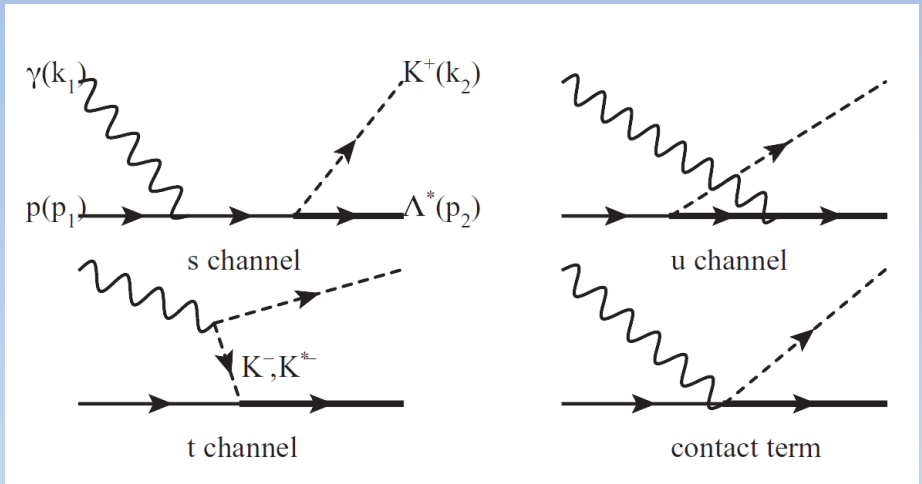

Reactions	$\gamma p \to K^+\Lambda^*$		$\gamma n \to K^0\Lambda^*$
σ	$\sim 900\ nb$	>>	$\sim 30\ nb$

Cross sections of *Neutron* much smaller than *Proton*

?

S. Nam et al. Phys. Rev. D, 71, 114012 (2005)

Cross Section photoproduction

LEPS Results

- Show both forward and backward angle differential cross sections on *Proton*.
- Enhancement close to threshold is interpreted as a resonance structure.
- Very small cross sections on *Neutron* from indirect measurement.

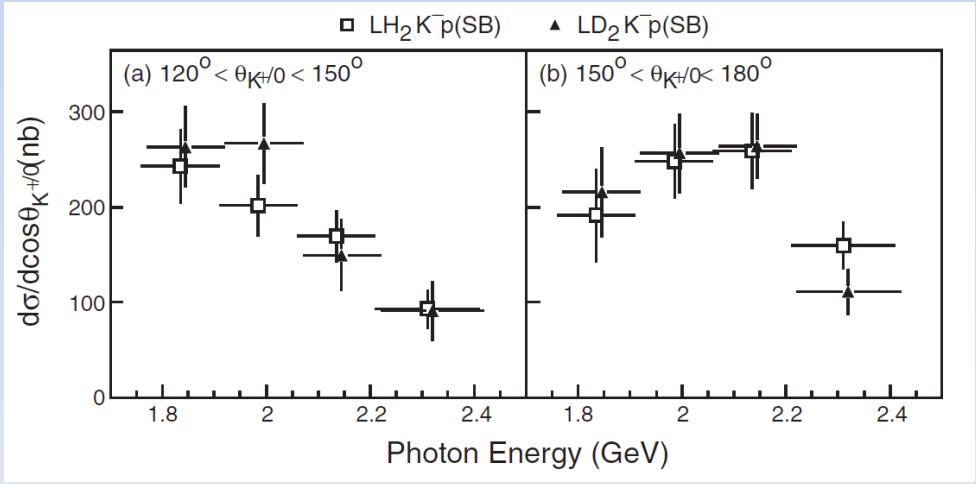

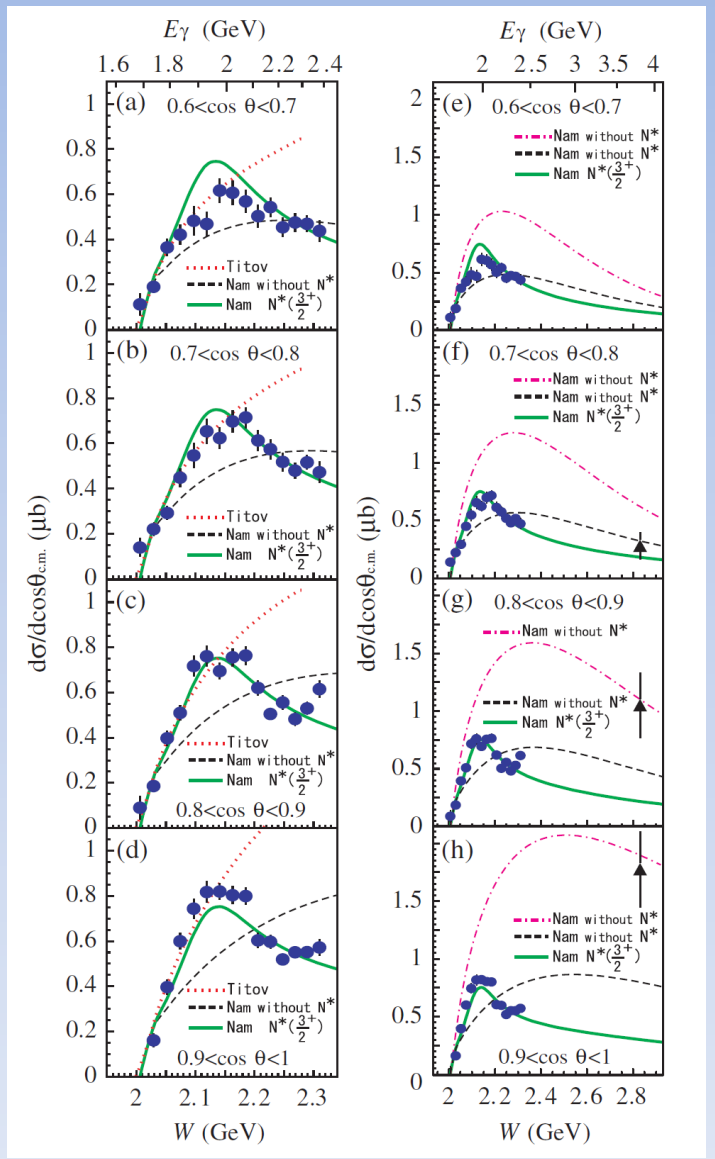

Decay Angle photoproduction

Gottfried-Jackson frame

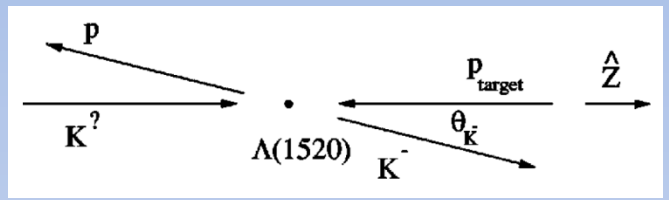

Decay angle distribution

m_z=1/2 m_z=3/2 interference

$$f(\theta^{GJ}_{K^-}) = \alpha\left(\frac{1}{3} + cos^2\theta^{GJ}_{K^-}\right) + \beta\left(1 - cos^2\theta^{GJ}_{K^-}\right) + \gamma\left(cos\theta^{GJ}_{K^-}\right)$$

Λ* $J^P = 3/2^-$	m_z=1/2	m_z=3/2	β/α
N(1/2 $^+$)K (0 $^-$)	Y	N	0
N(1/2 $^+$) K*(1 $^-$)	Y	Y	3/1

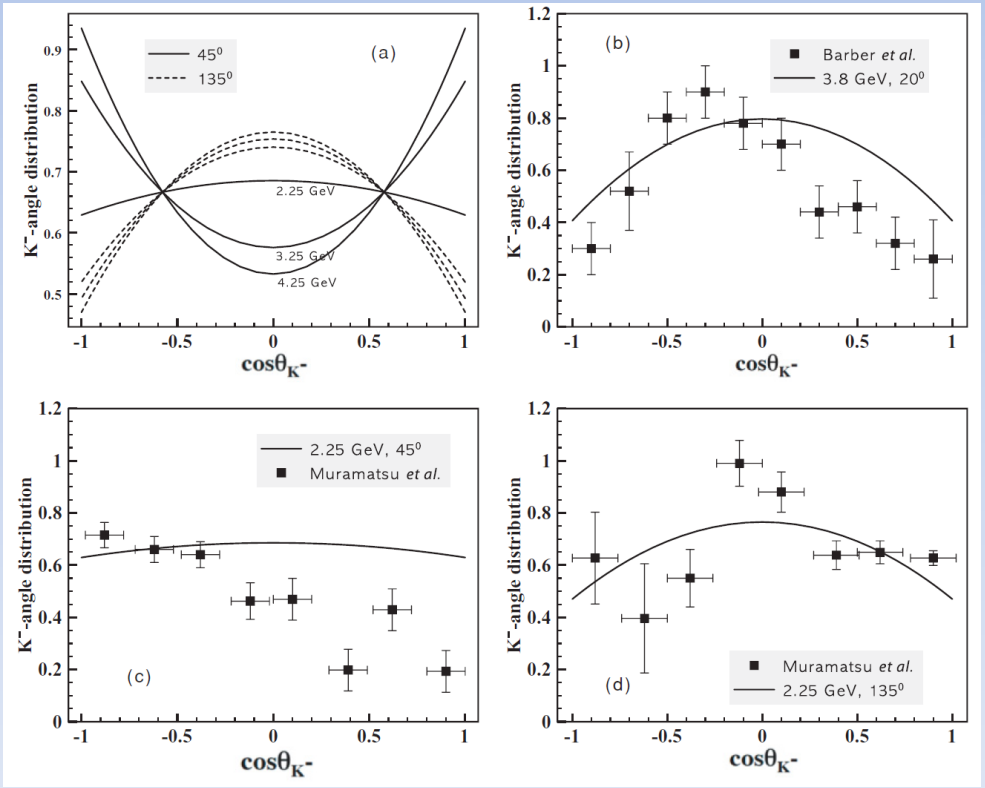

Decay angle distribution is related to production mechanism.

Decay Angle photoproduction

θ_K^{CM}	forward	backward

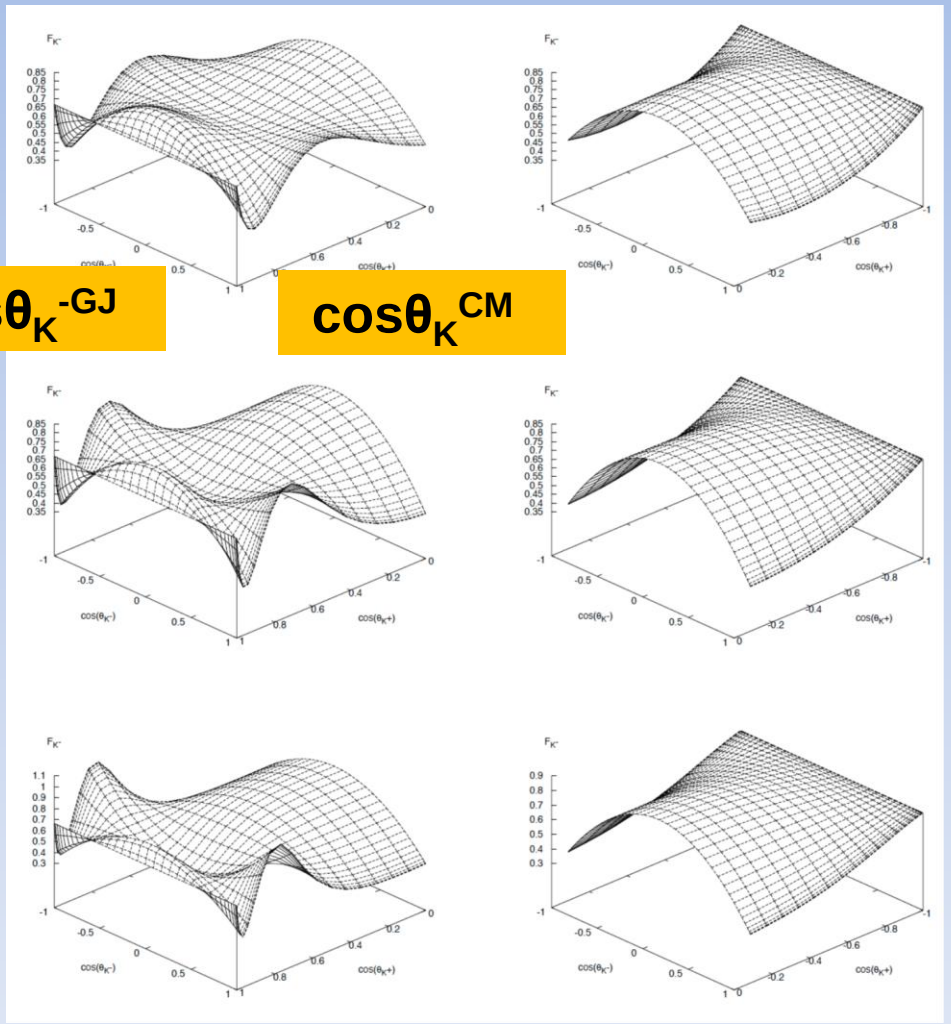

S. Nam et al. Phys. Rev. C, 81, 055206 (2010)

Reaction Channels

exclusive

deuteron target

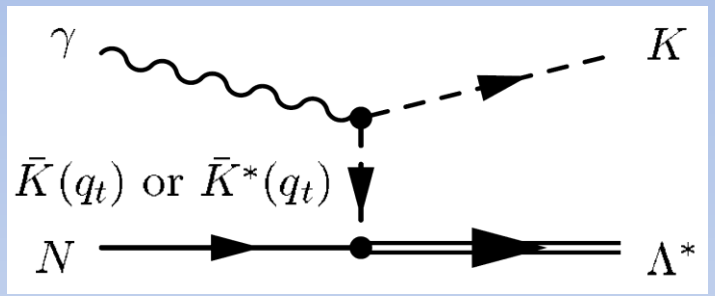

$\gamma p(n) \rightarrow K^+ \Lambda^* (n)$ ***Proton***

$\gamma n(p) \rightarrow K^0 \Lambda^* (p)$ ***Neutron***

$(\Lambda^* \rightarrow p\, K^-\, , K^0 \rightarrow K_s \rightarrow \pi^+ \pi^-)$

eg3 run

- **Photon beam** — **electron beam 5.77 GeV, tagged photon energy 1.15 < E < 5.5 GeV, 30 nA**
- **Target** — **40 cm upstream, LD^2**
- **TriggerTagger** — **4.5 < E < 5.5 GeV, STxTOF (3 sectors and prescaled 2 sectors)**
- **Torus field** — **optimized to -1980 A, negative charged particles outbending**
- **Run period** — **12/06/2004 – 01/31/2005, 29 days of production on LD^2 target**
- **Data** — **4.2 billion physics events, 32 TB raw data, average 2.7 tracks/event**

Correction and Cuts Applied

Correction and cut name	experiment	simulation
Beam trip cut	Y	N
Eloss correction	Y	Y
Momentum correction	Y	N
Photon energy correction	Y	N
Fiducial cut	Y	Y
SC occupancy cut	Y	Y
DC wire efficiency correction	N	Y
Untriggered tagger T-counter correction	Y	N
Trigger efficiency correction	Y	N
Trigger condition cut	Y	Y
Vertex Z cut	Y	Y
Momentum cut	Y	Y

Invariant Mass of pK^-

Proton ***Neutron***

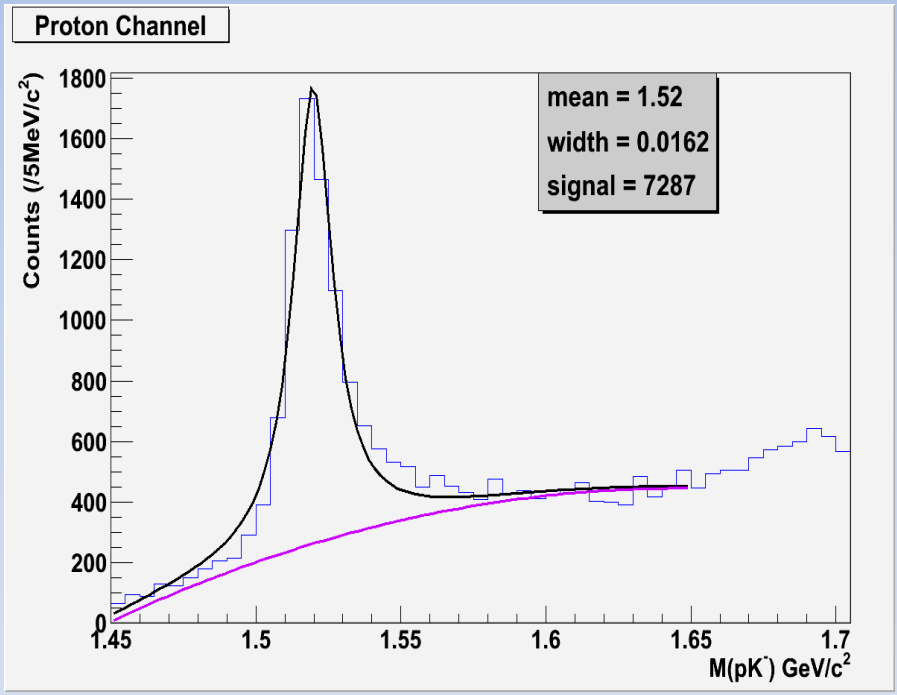

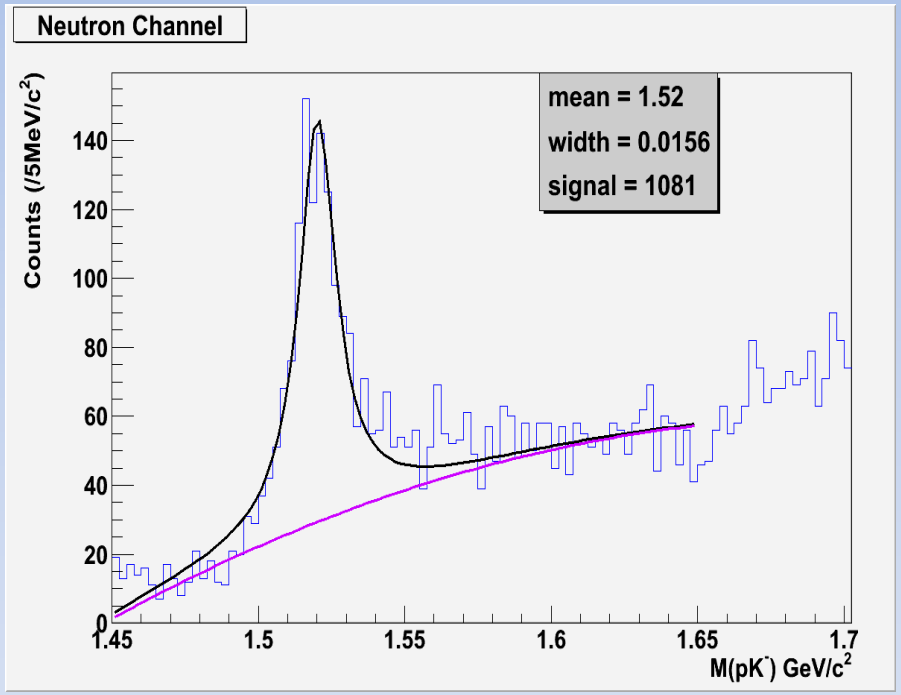

Proton

Invariant Mass of K^+K^-

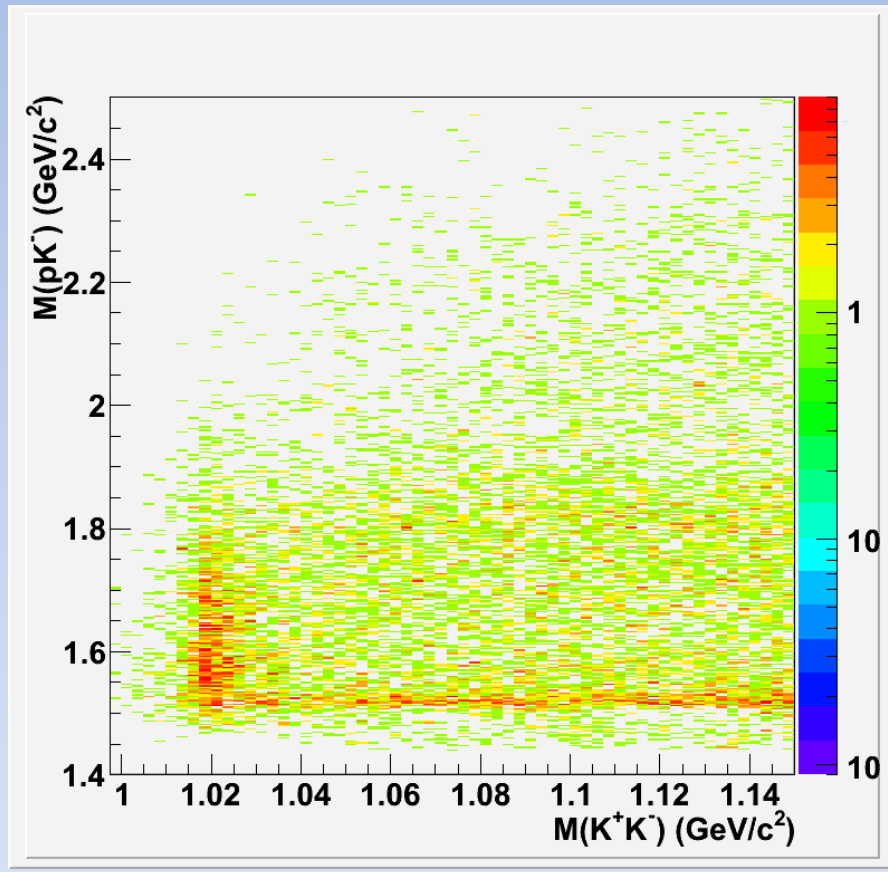

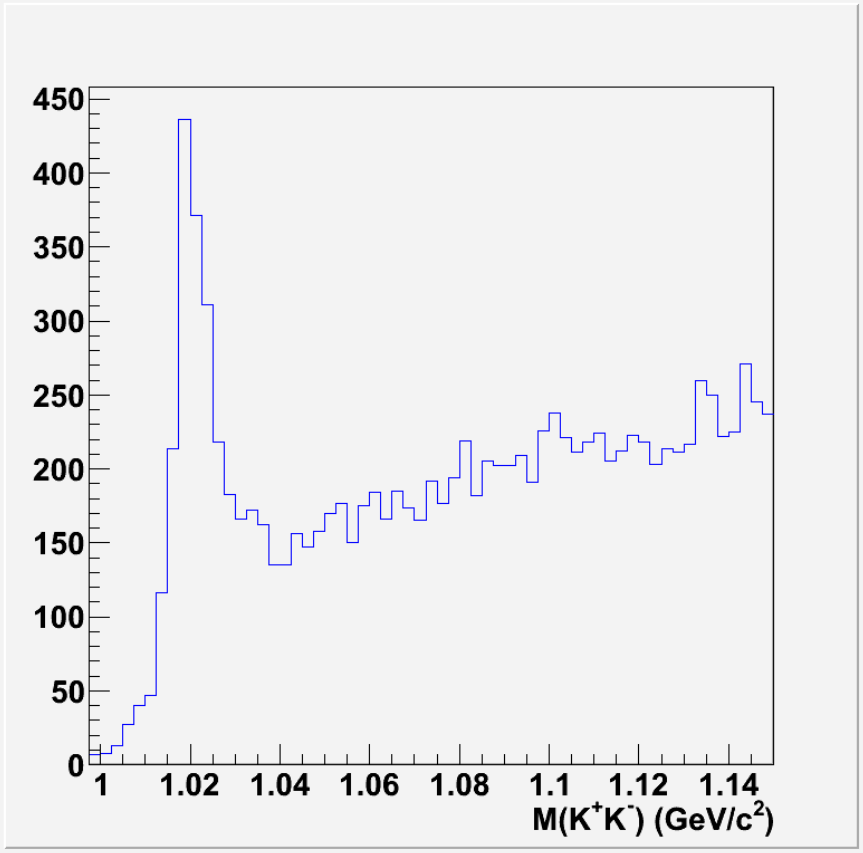

Proton

Invariant Mass of K^+K^-

$E_\gamma < 2.25$ GeV

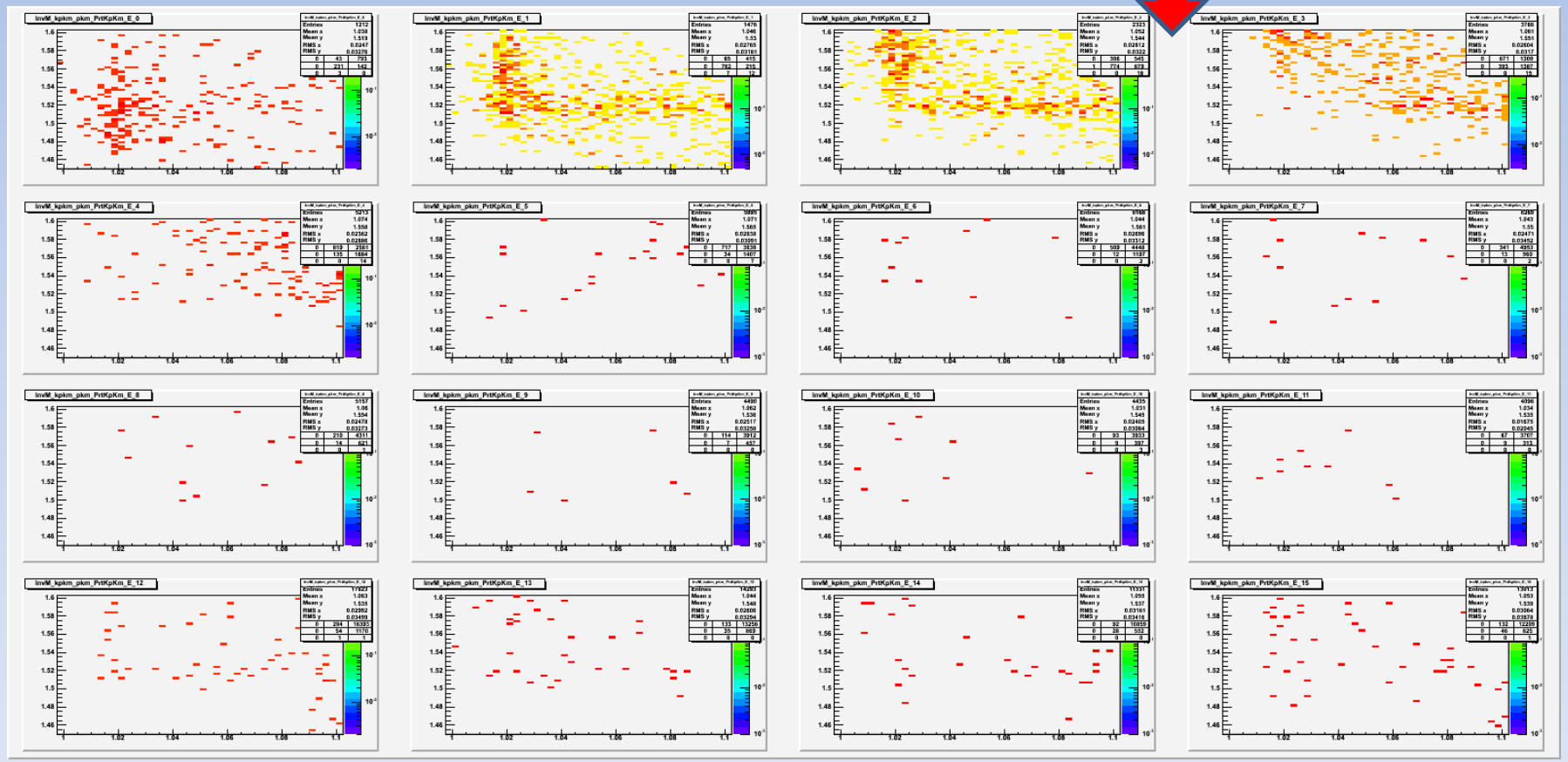

Proton

Kinematic Distribution

$1.5 < E_\gamma < 5.5$ GeV
16 bins, bin width 250 MeV

$0.25 < t^* = -(t-t_0) < 2.5$ GeV^2
6 bins, bin width varies

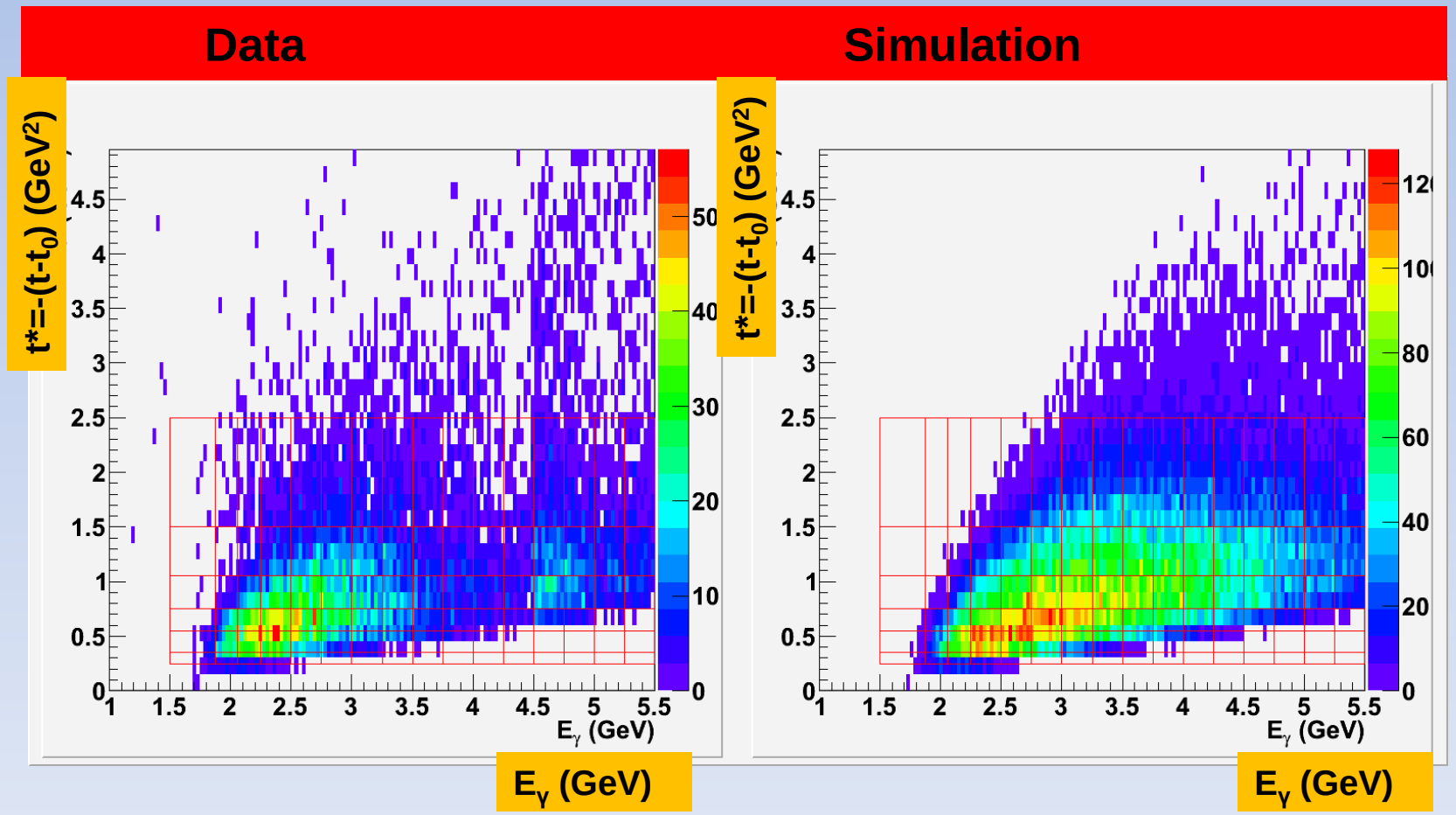

Neutron

Kinematic Distribution

$1.5 < E_\gamma < 5.5$ GeV
6 bins, bin width varies

$0.0 < t^* = -(t-t_0) < 2.5$ GeV^2
6 bins, bin width varies

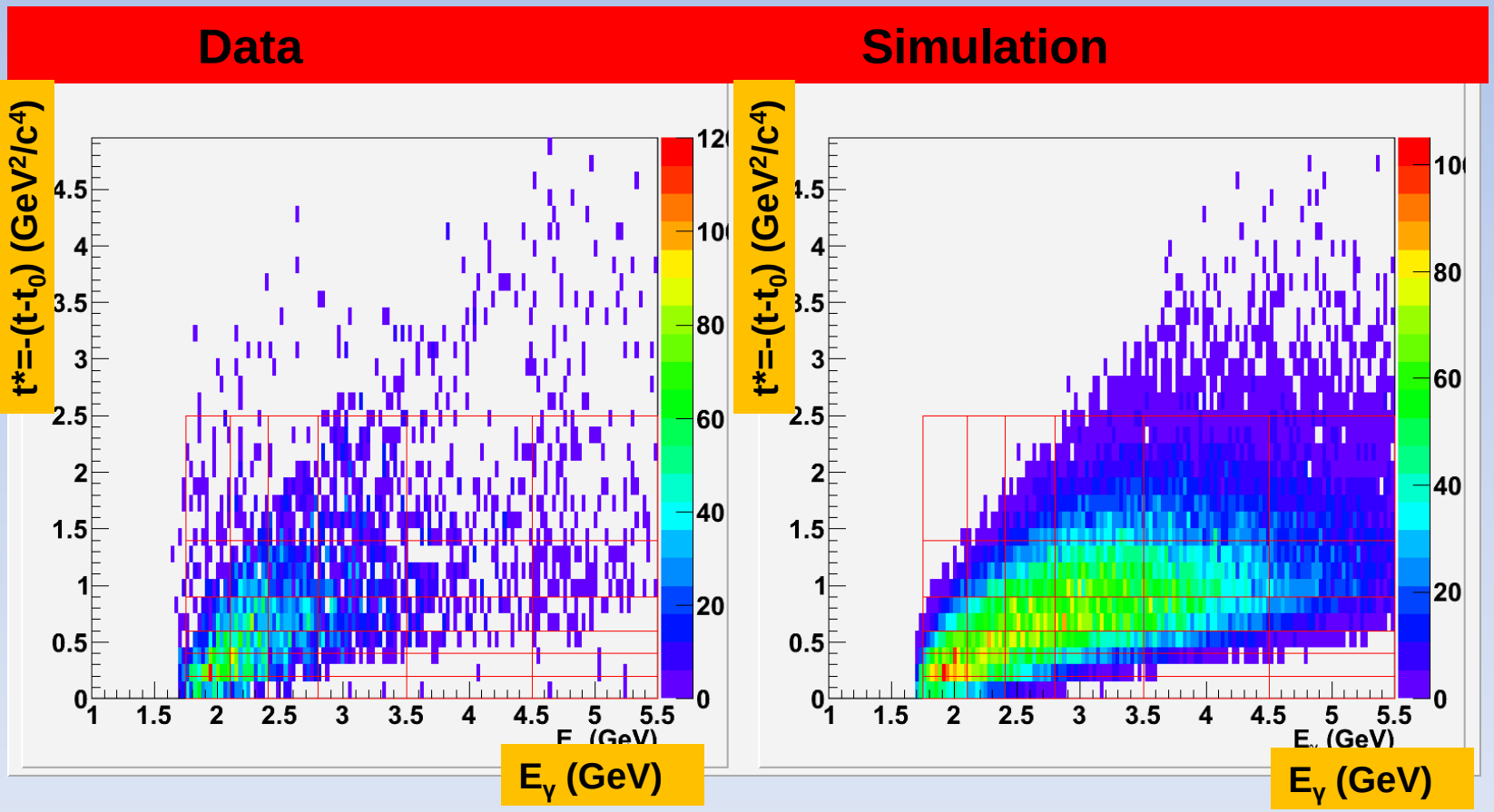

Proton

Preliminary

Differential Cross Section

dσ/dt*

- $1.5 < E_g < 5.5$ GeV
16 bins, bin width 250 MeV

- Fit with function of $\alpha e^{-\beta t^*}$

- Extrapolate the function and integrate over t* to obtain total cross sections

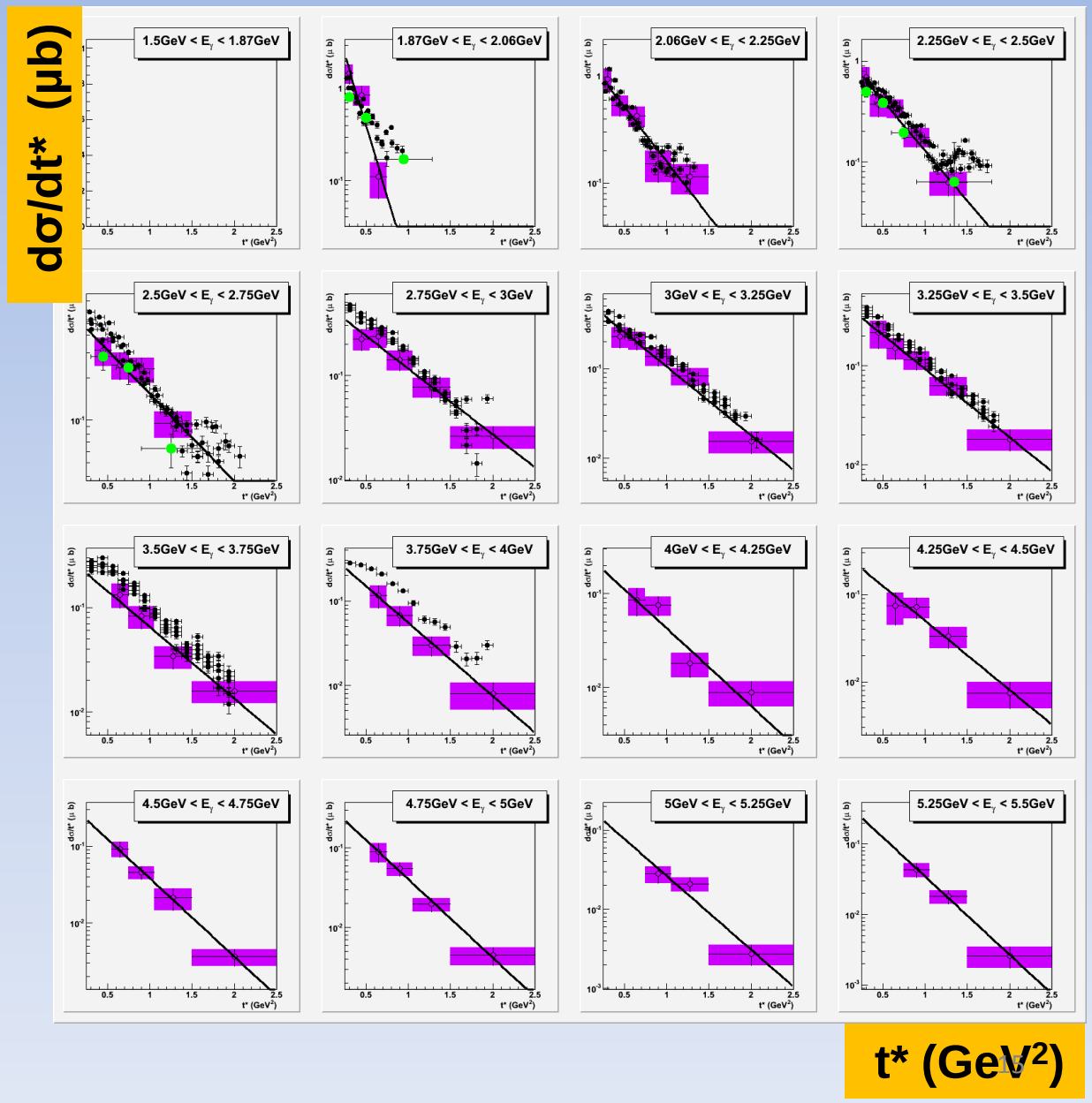

Neutron

Preliminary

Differential Cross Section

dσ/dt*

- $1.5 < E_g < 5.5$ GeV
6 bins, bin width varies.

- Fit with function of $\alpha e^{-\beta t^*}$

- Extrapolate the function and integrate over t* to obtain total cross sections

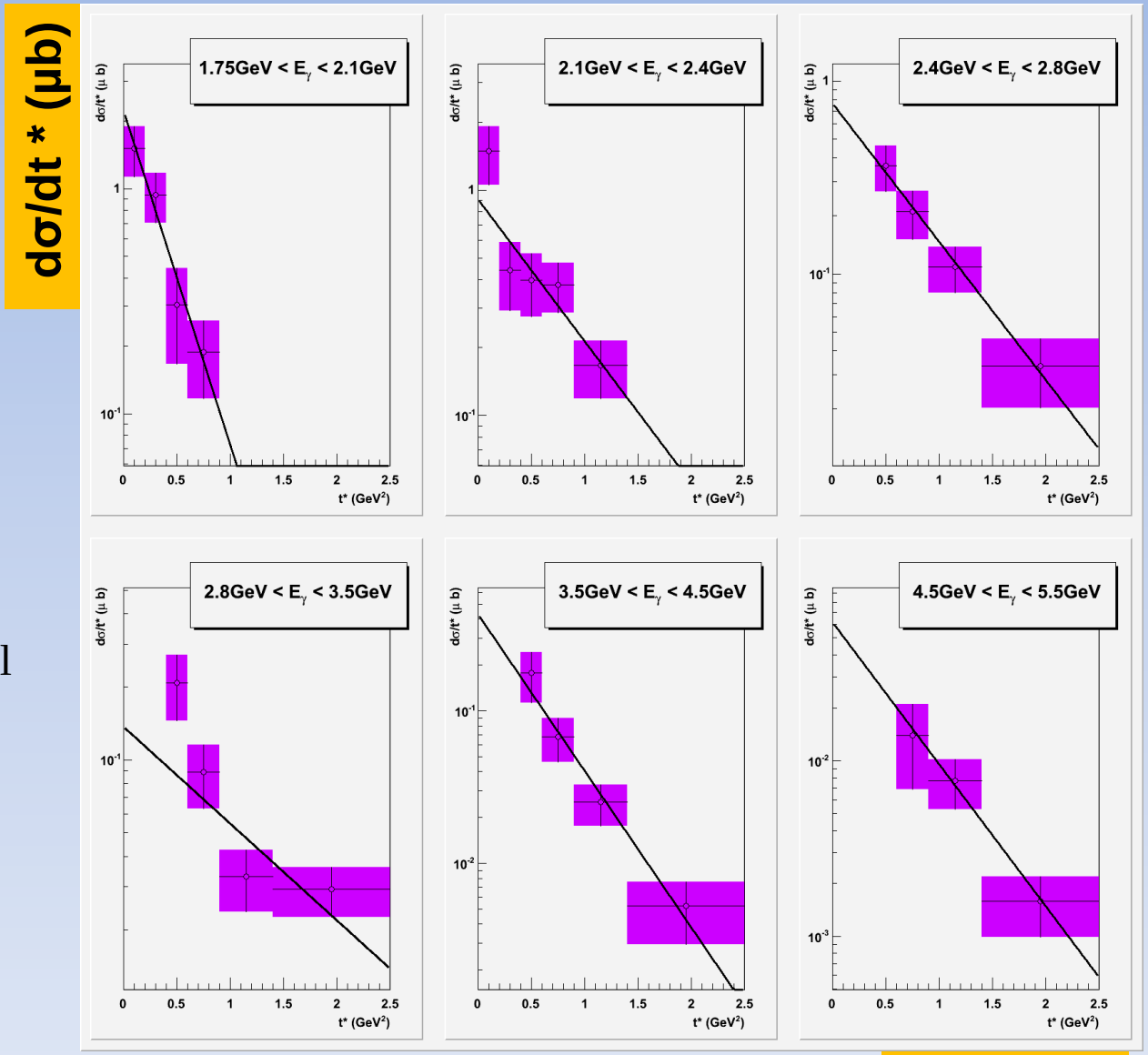

Preliminary

t-slope

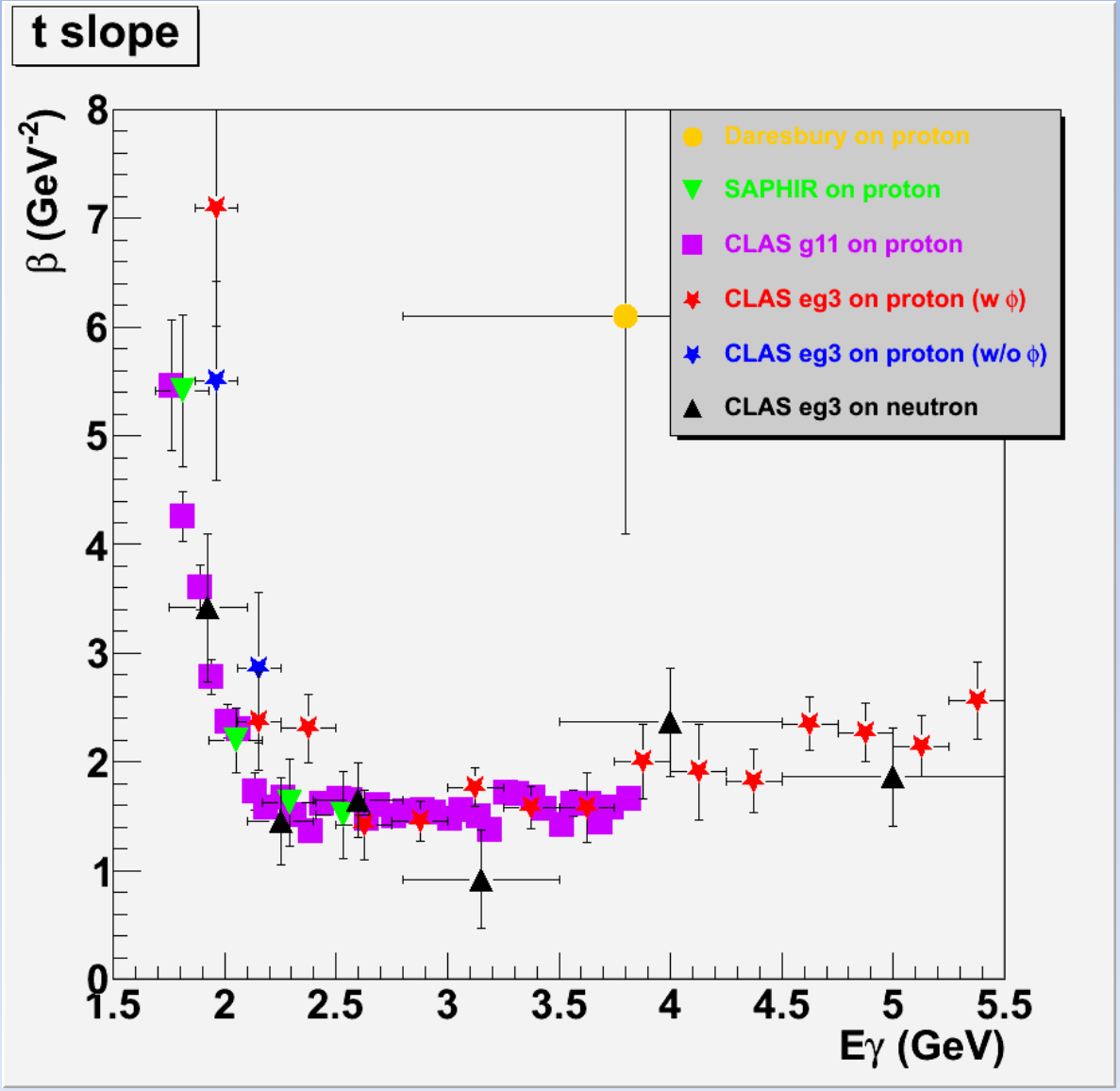

Preliminary

Total Cross Section

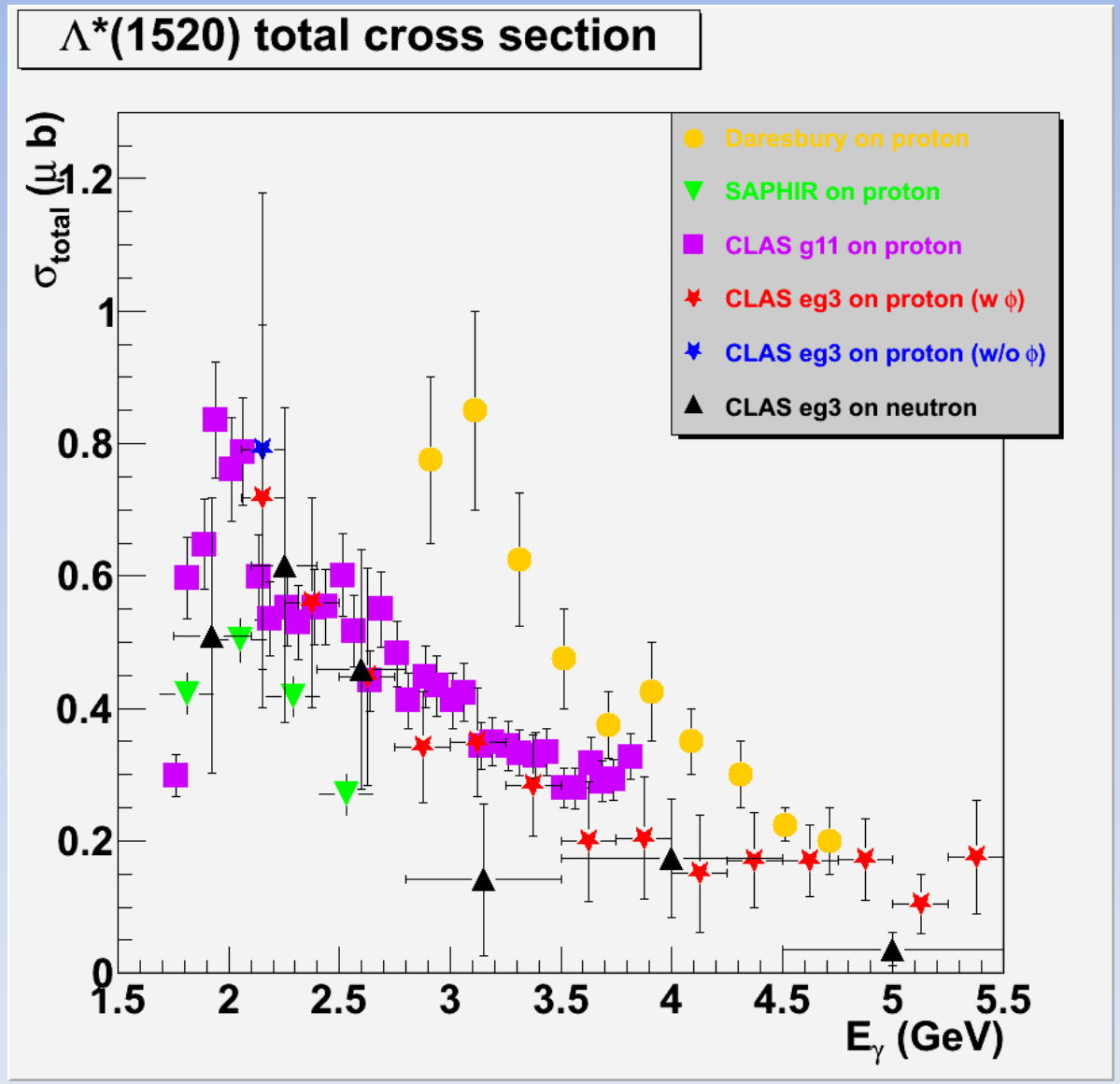

Proton

Kinematic Distribution

$1.5 < E_\gamma < 5.5$ GeV
16 bins, bin width 250 MeV

$40 < \theta_K^{CM} < 120^o$
6 bins, bin width varies

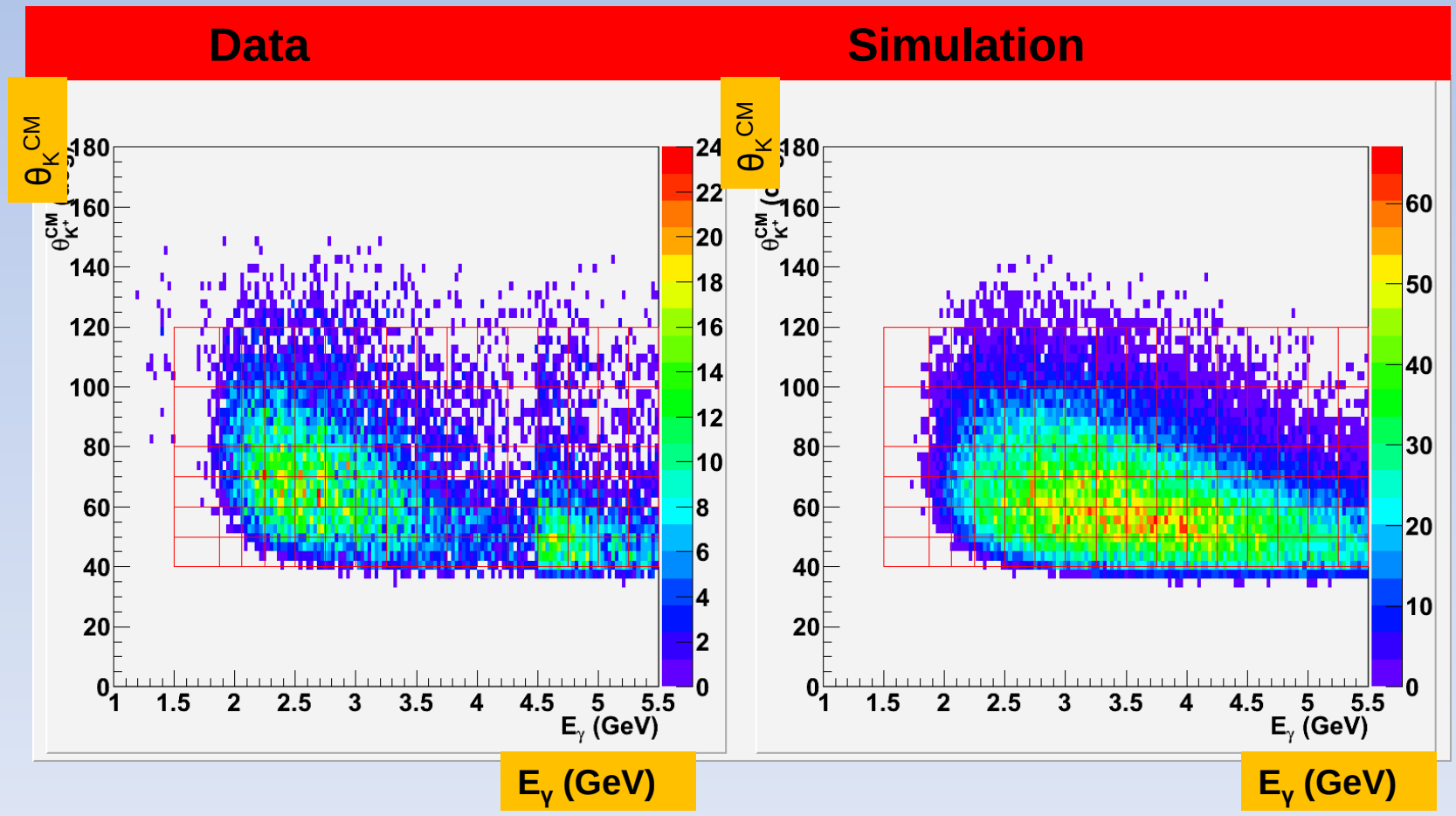

Neutron

Kinematic Distribution

$1.5 < E_\gamma < 5.5$ GeV
6 bins, bin width varies

$30 < \theta_K^{CM} < 120^o$
6 bins, bin width varies

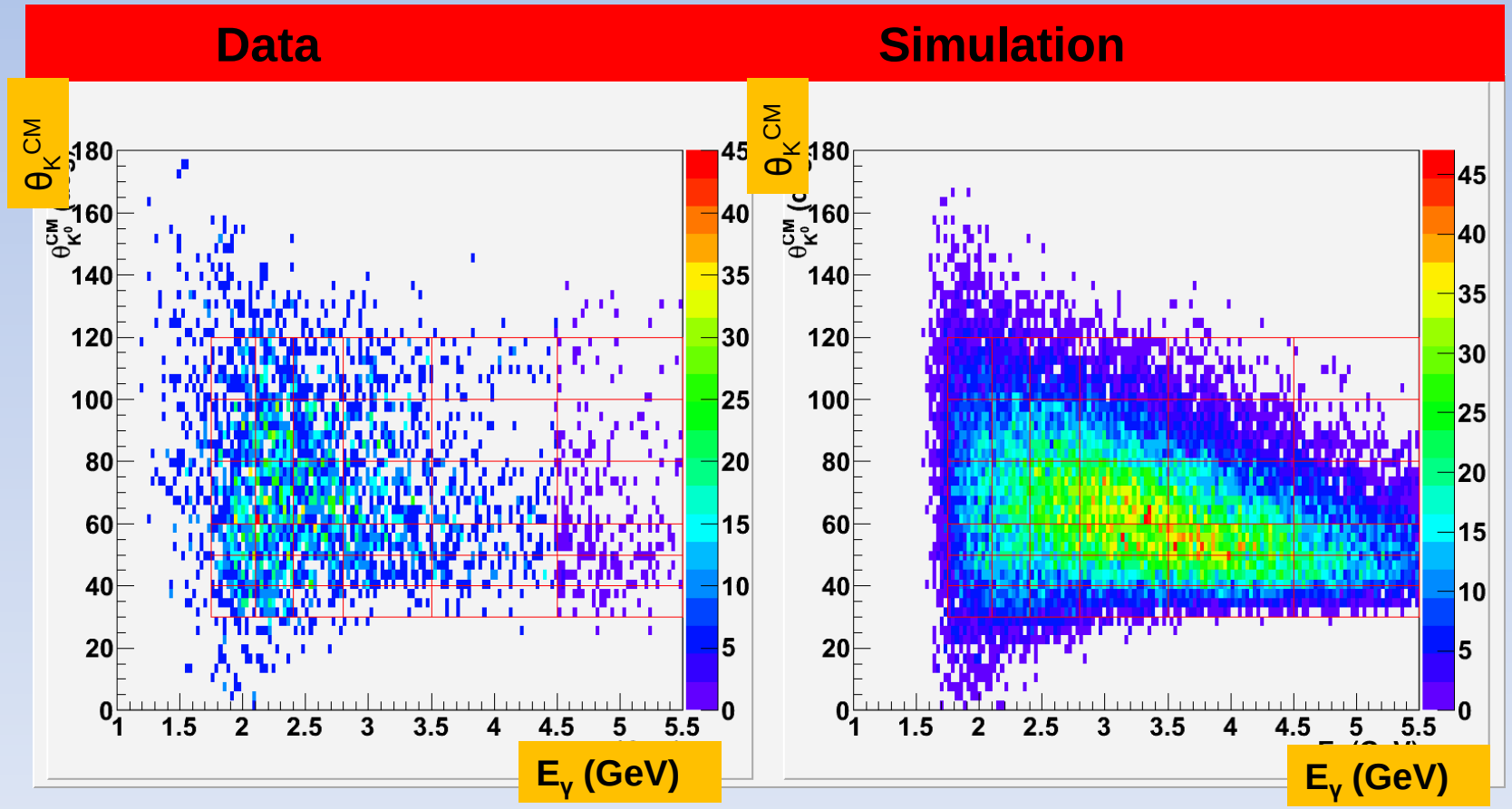

Proton

Preliminary

Differential Cross Section

$d\sigma/d\theta_K^{CM}$

- $40^o < \theta_K^{CM} < 120^o$
6 bins, bin width varies

- No sign of resonance structure within the statistics

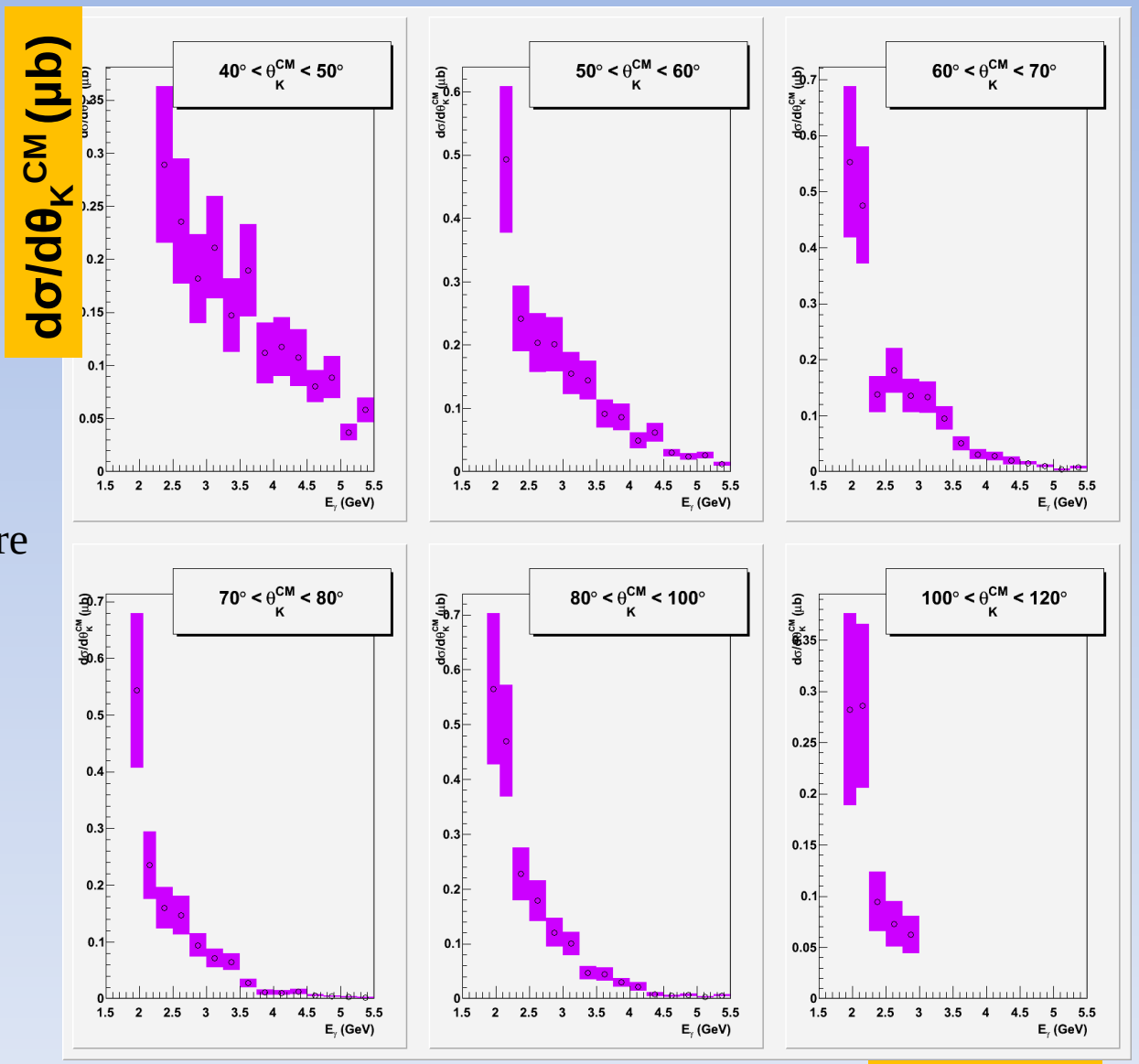

Neutron

Preliminary

Differential Cross Section

$d\sigma/d\theta_K^{CM}$

- $20^o < \theta_K^{CM} < 120^o$

6 bins, bin width varies

- No sign of resonance structure within the statistics

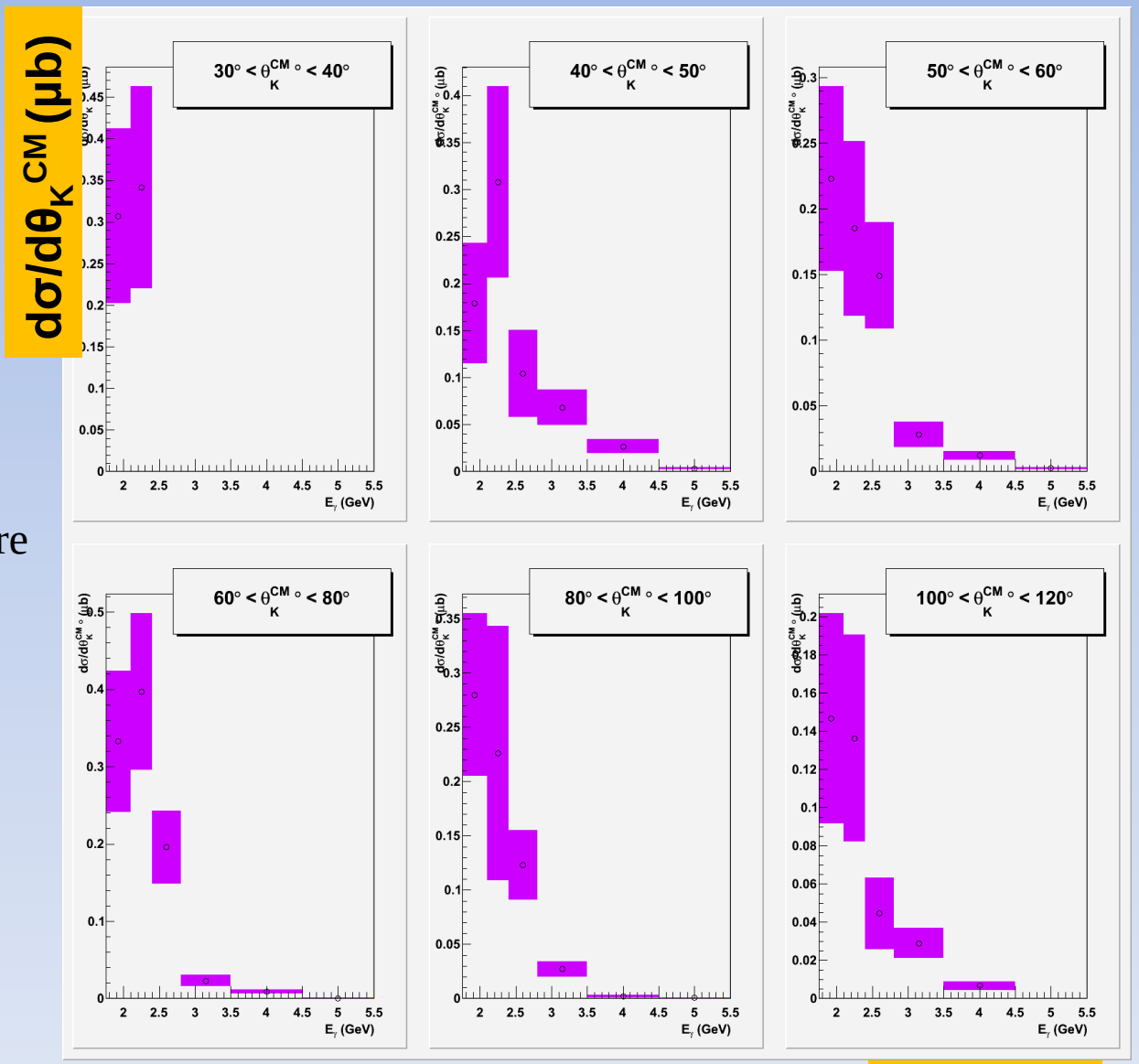

E_γ (GeV)

Preliminary

Proton

Decay Angle Distribution

$d\sigma/dcos\theta_K^{-GJ}$

- $1.5 < E_g < 5.5$ GeV
16 bins, bin width 250 MeV

- Mixture of K and K* exchange

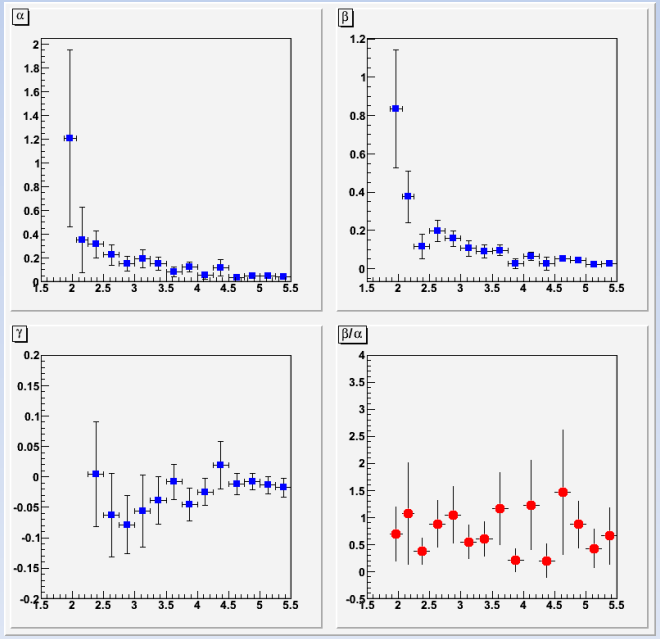

$d\sigma/d\theta_K^{-GJ}$ (μb)

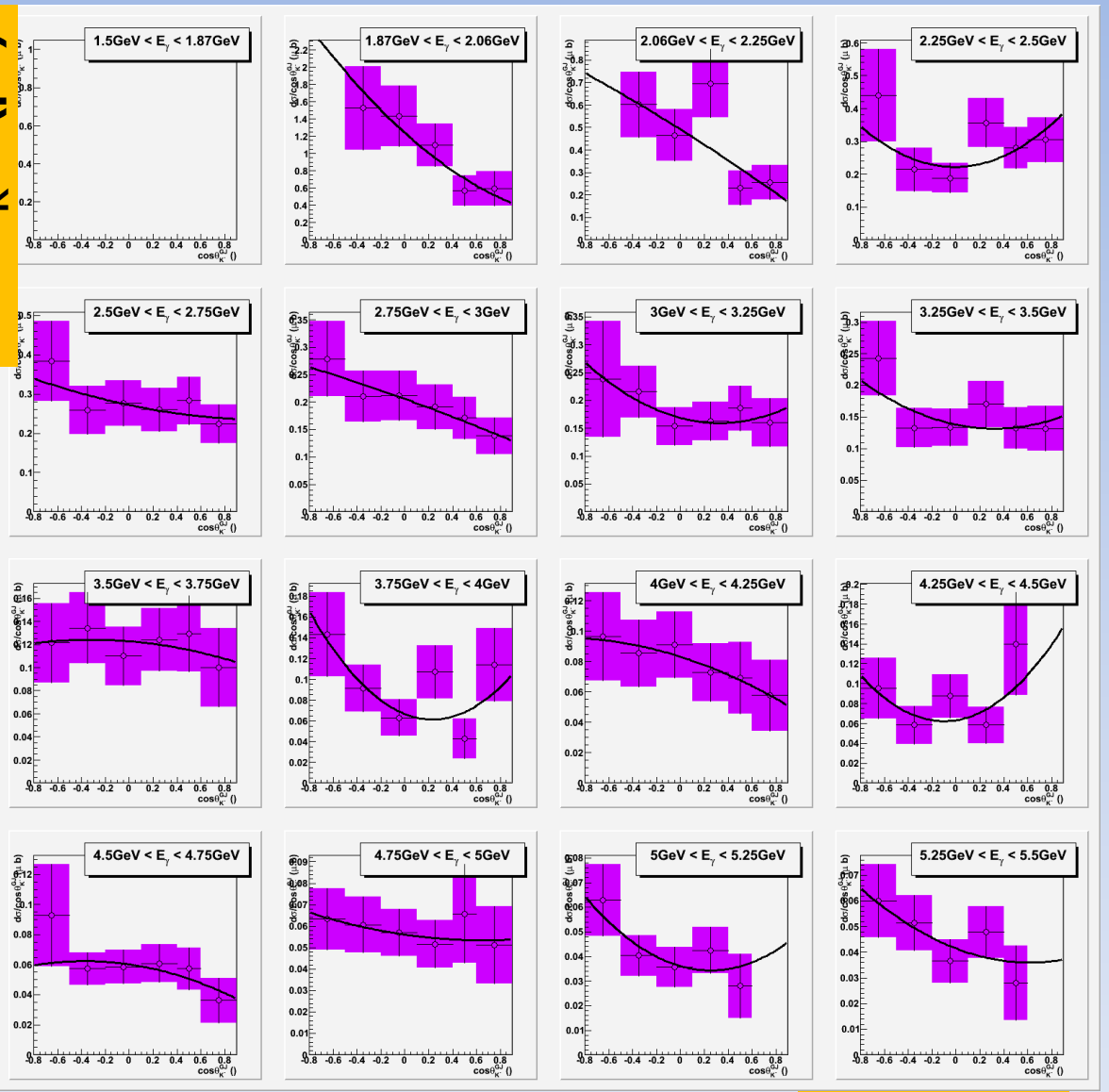

$cos\theta_K^{-GJ}$

Neutron

Preliminary

Decay Angle Distribution

$d\sigma/d\cos\theta_K^{-GJ}$

- $1.5 < E_g < 5.5$ GeV
6 bins, bin width varies

- Mixture of K and K* exchange

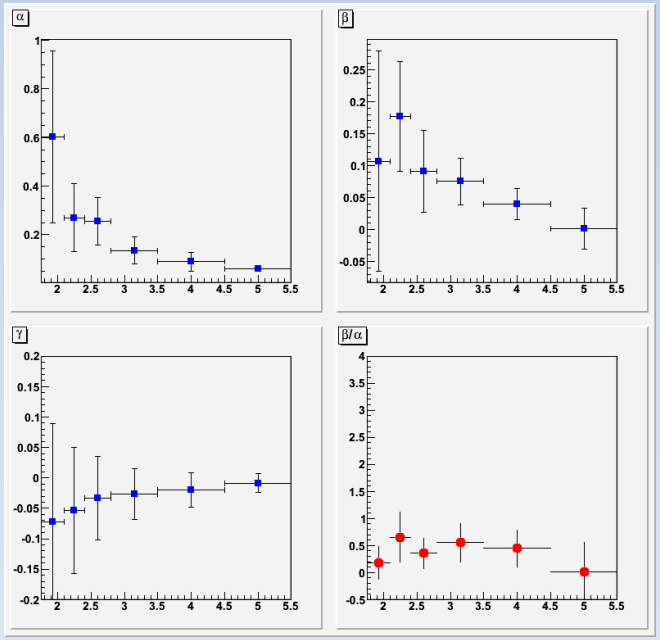

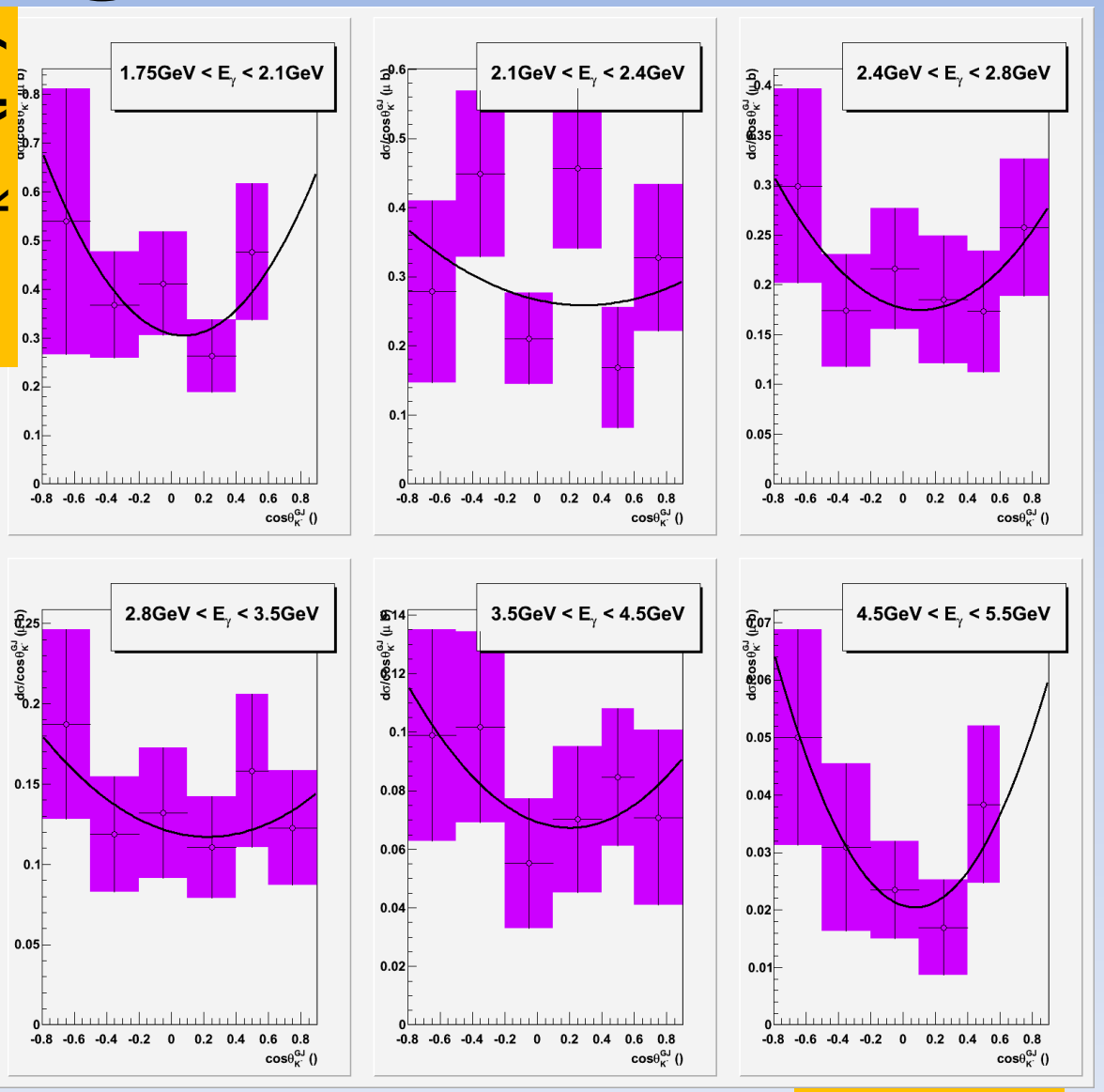

$\cos\theta_K^{-GJ}$

Proton

Preliminary

Decay Angle Distribution

$d\sigma/d\cos\theta_K^{-GJ}$

Mixture of K and K* exchange

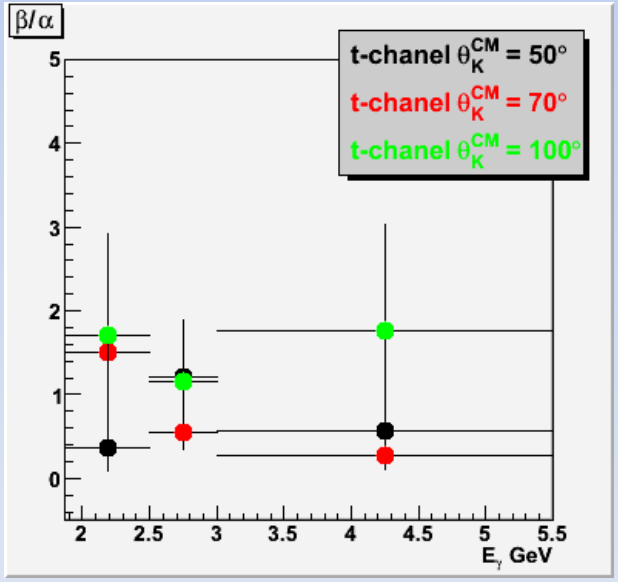

E_γ = 2.185 2.75 4.35 GeV

$d\sigma/d\theta_K^{-CJ}$ (μb)

θ_K^{CM} = 50 70 100 DEG

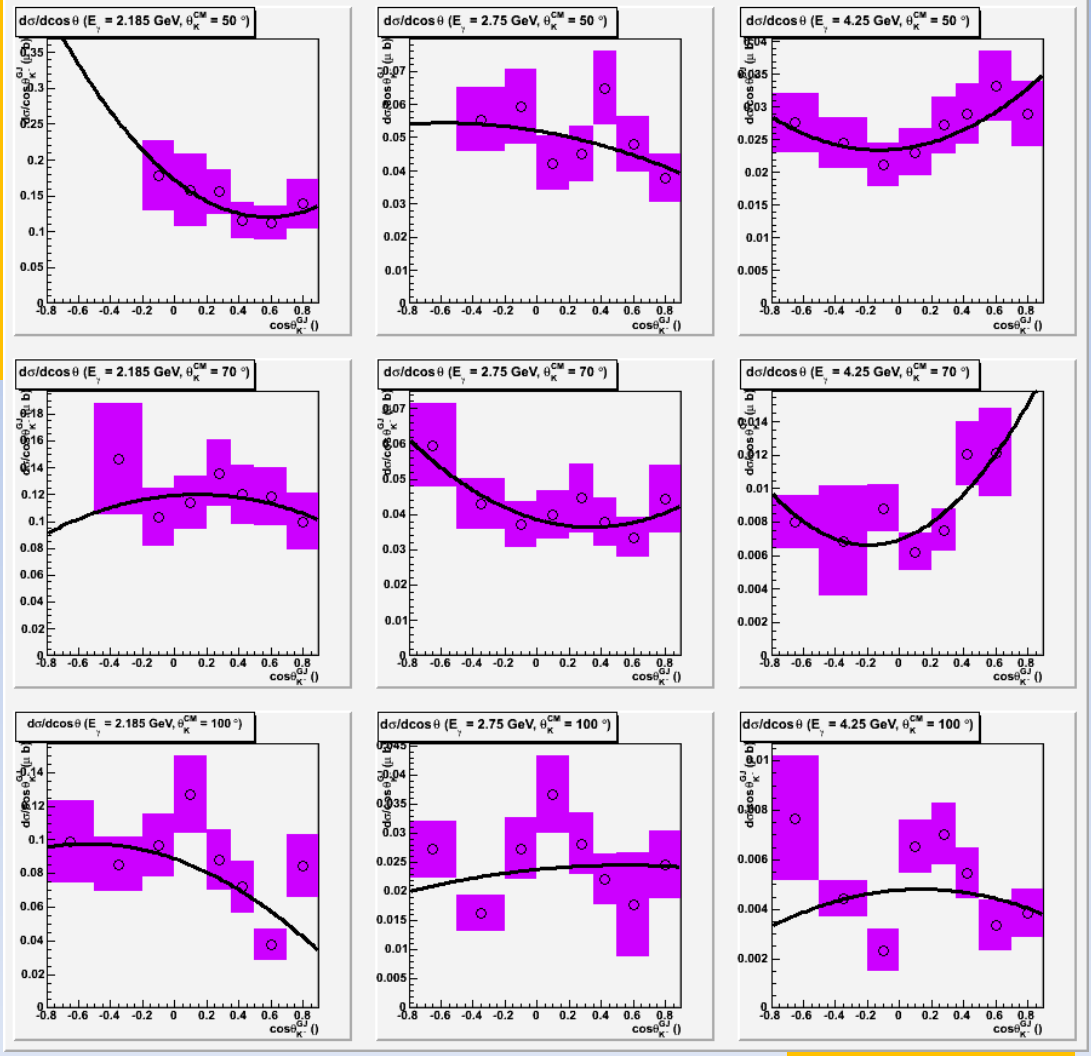

$\cos\theta_K^{-GJ}$

Neutron

Preliminary

Decay Angle Distribution

$d\sigma/d\cos\theta_K^{-GJ}$

Mixture of K and K* exchange

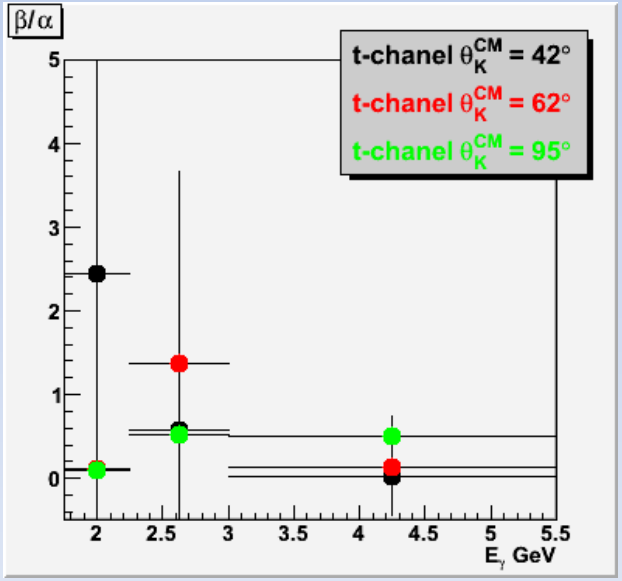

E_γ = 2.0 2.625 4.35 GeV

$d\sigma/d\theta_K^{-CJ}$ (μb)

θ_K^{CM} = 42 62 95 DEG

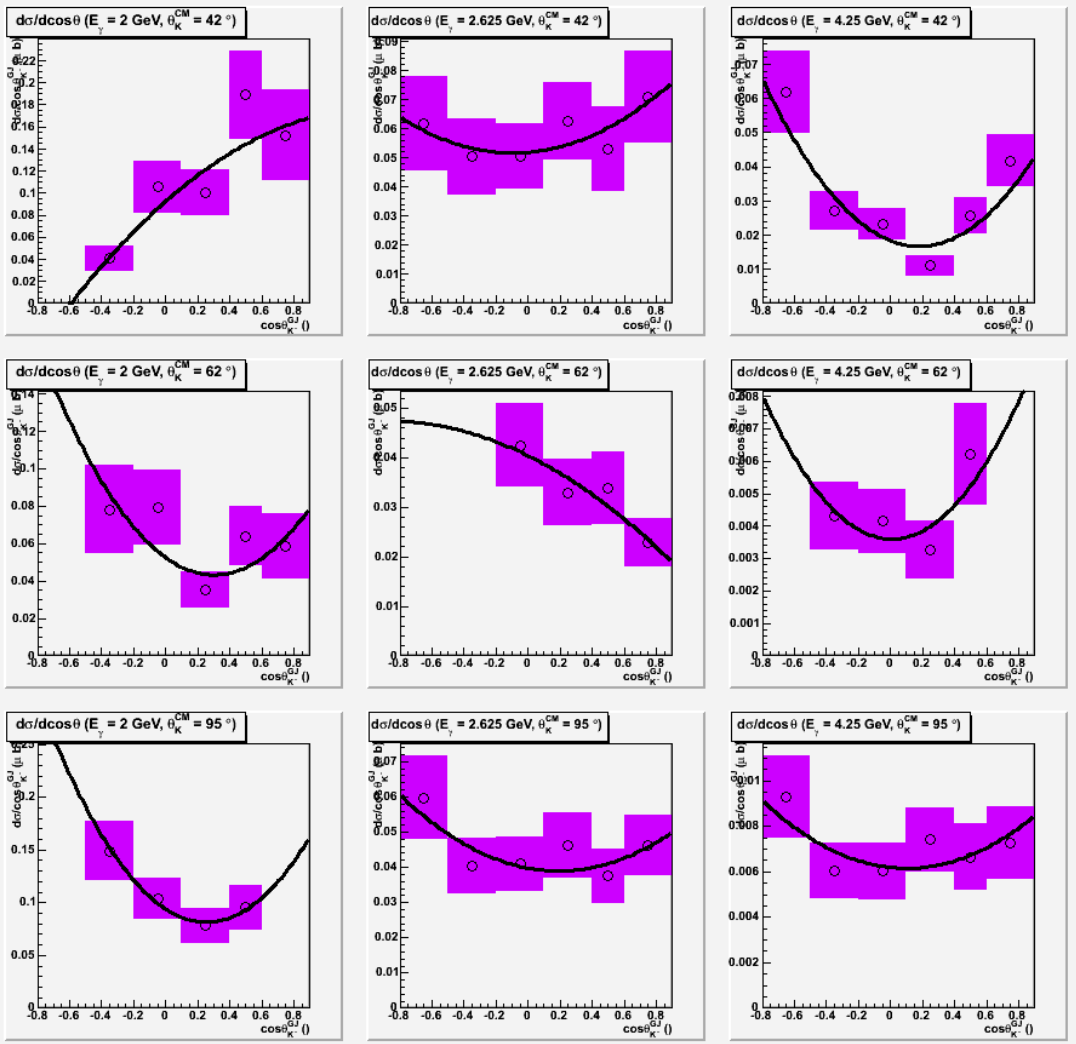

$\cos\theta_K^{-GJ}$

Summary

- The $\Lambda^*(1520)$ differential and total cross sections up to 5.5 GeV on ***Proton*** are extracted. The total cross section is in good agreement with the world data.
- The $\Lambda^*(1520)$ differential and total cross sections on ***Neutron*** are obtained for the first time. The cross section is about 70% of the proton channel result, which is much larger than what the theory predicted.
- There is no sign of resonance structures at the covered forward kaon angles.
- $\Lambda^*(1520)$ decay angle distributions in Gottfried-Jackson frame show complicated structures indicating that both K and K* exchanges contribute to the two reaction channels.

Backup

Existing Data electroproduction

- Electroproduction of Λ* off ***Proton*** has been studied at DESY and CLAS
- CLAS data (S. Barrow, e1c) showed
  - Dominance of t-channel process confirmed
  - Decay angular distribution showed significant contribution from m_z=±1/2 spin projection

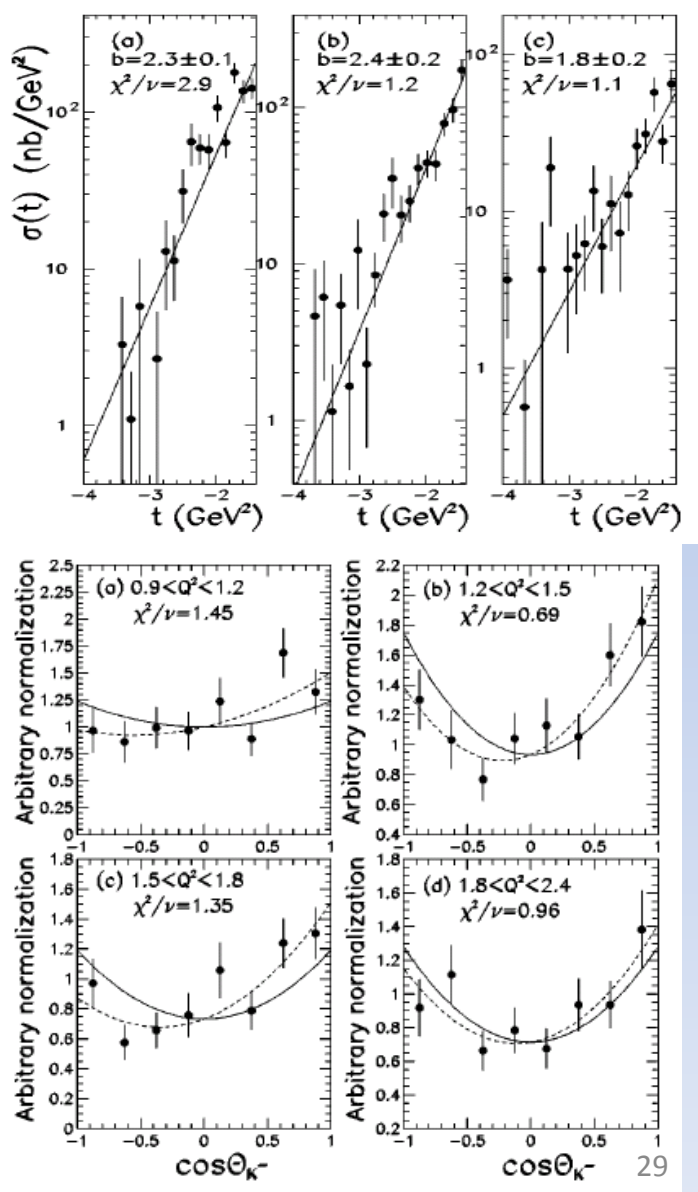

Photon Selection

Neutron

vertex time diff (ns)

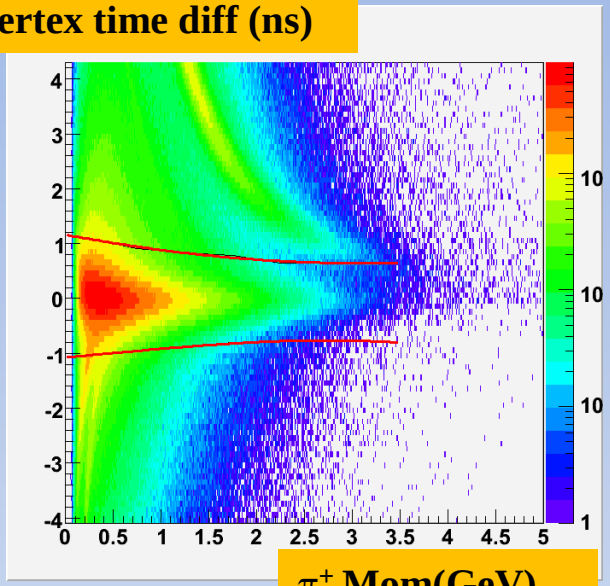

π^+ Mom(GeV)

vertex and tagger time diff (ns)

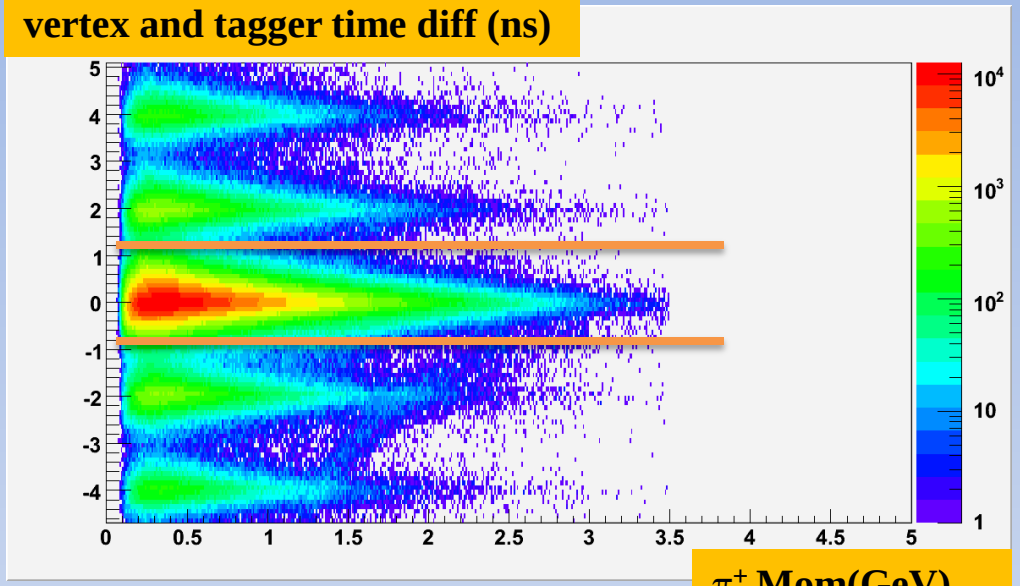

π^+ Mom(GeV)

vertex time diff (ns)

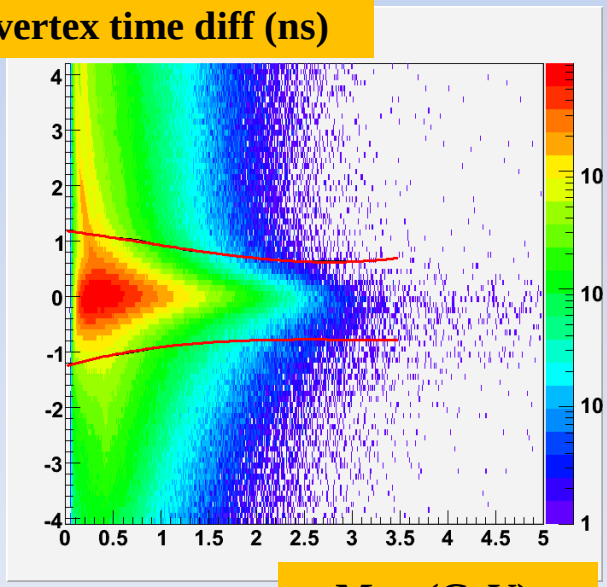

π^- Mom(GeV)

vertex and tagger time diff (ns)

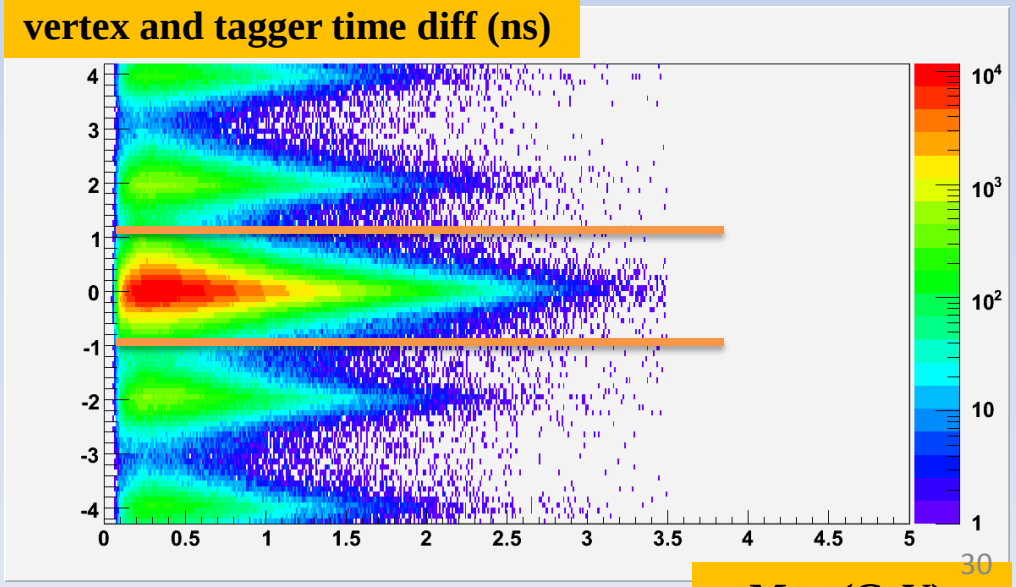

π^- Mom(GeV)

Event Selection

Proton

Positive Negative

τ

M^2

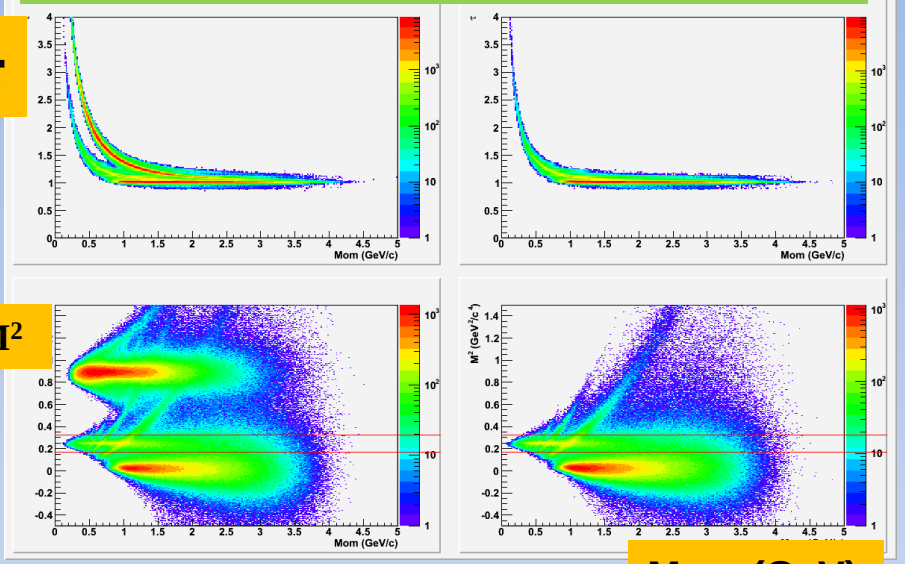

Particle timing

Cut misidentified pions

Mom (GeV)

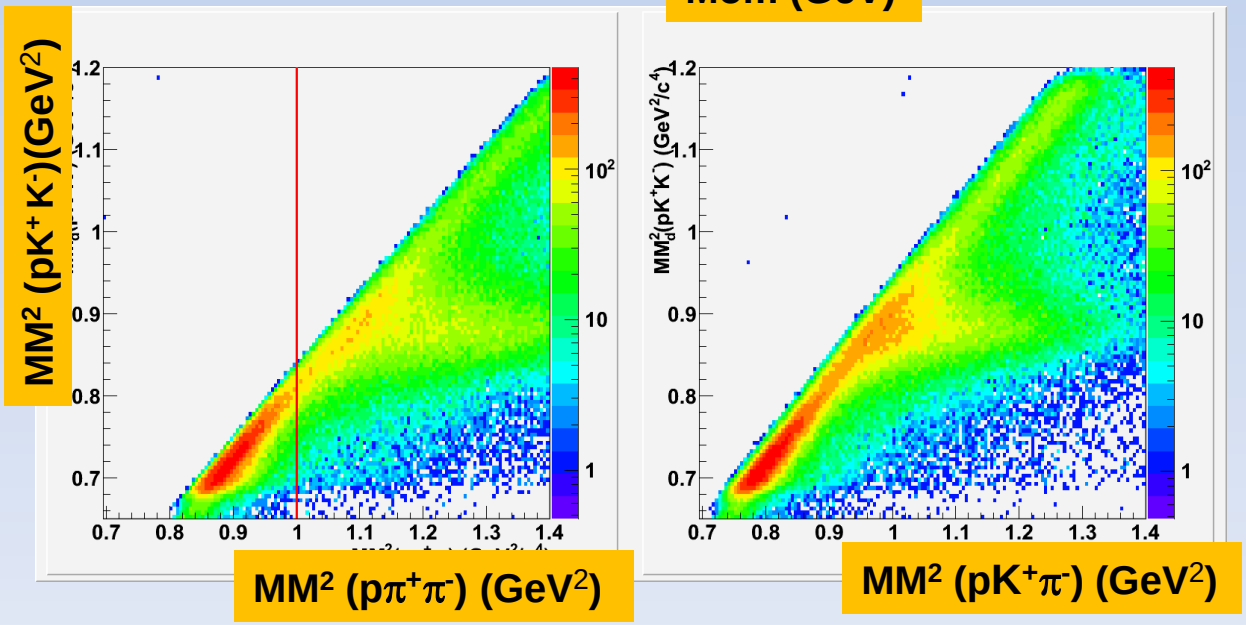

Before and after misid $\pi^+ \pi^-$ cut

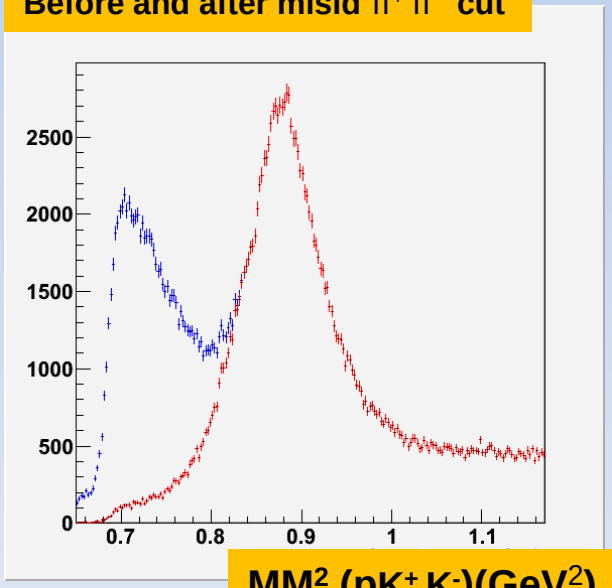

Event Selection

Neutron

Positive | Negative

τ

M^2

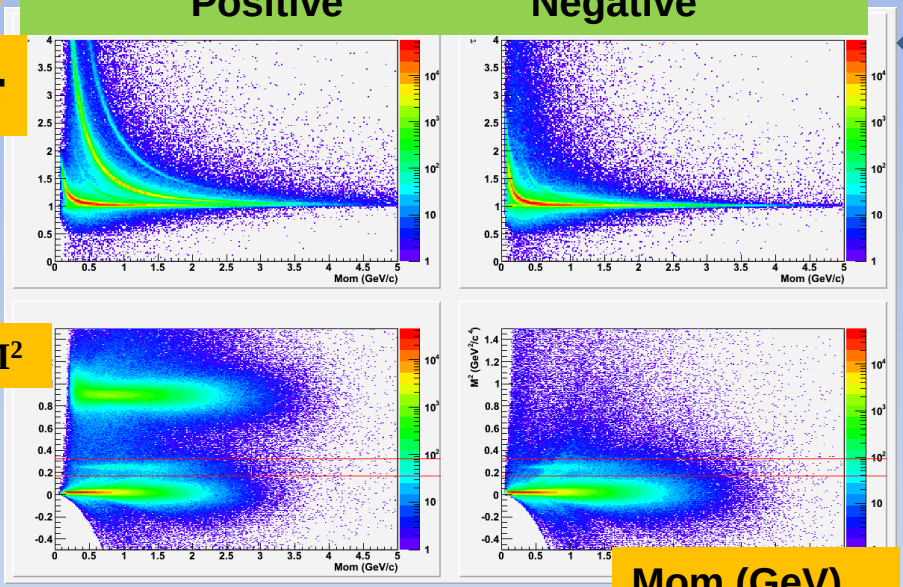

Particle timing

K_s cut

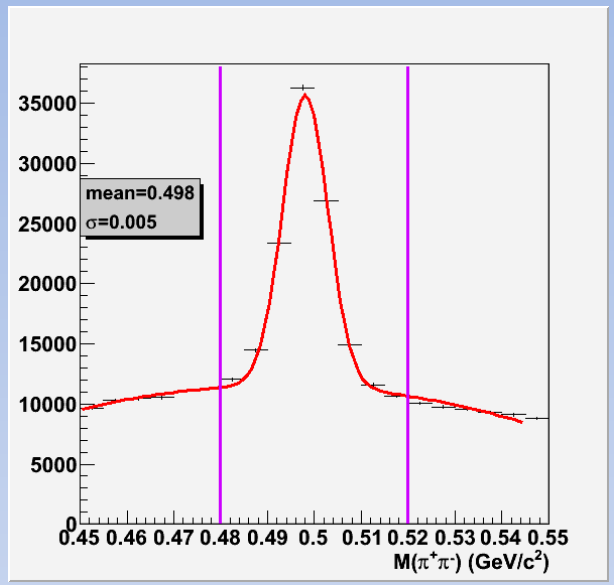

Mom (GeV)

Before K^0 cut

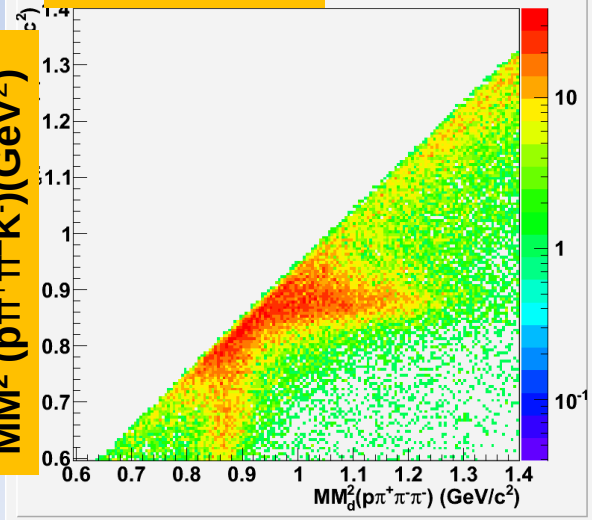

After K^0 cut

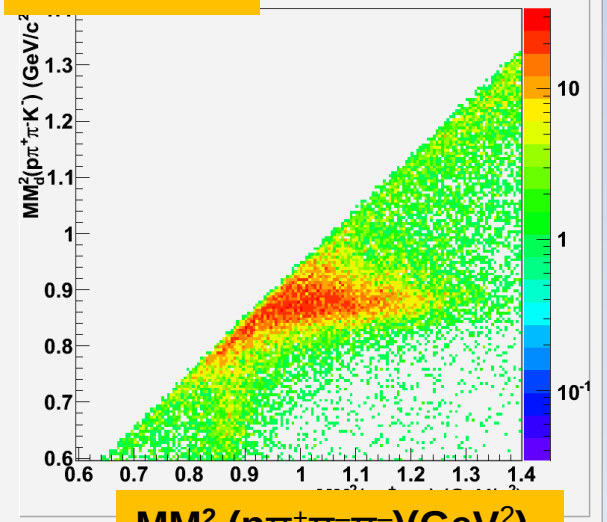

MM^2 $(p\pi^+\pi^-\pi^-)(GeV^2)$

Before and after K^0 cut

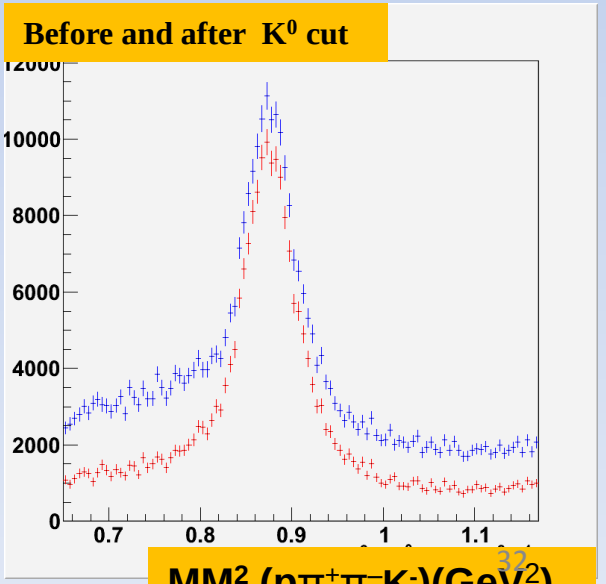

MM^2 $(p\pi^+\pi^-K^-)(GeV^2)$

Proton

Missing Nucleon Mass

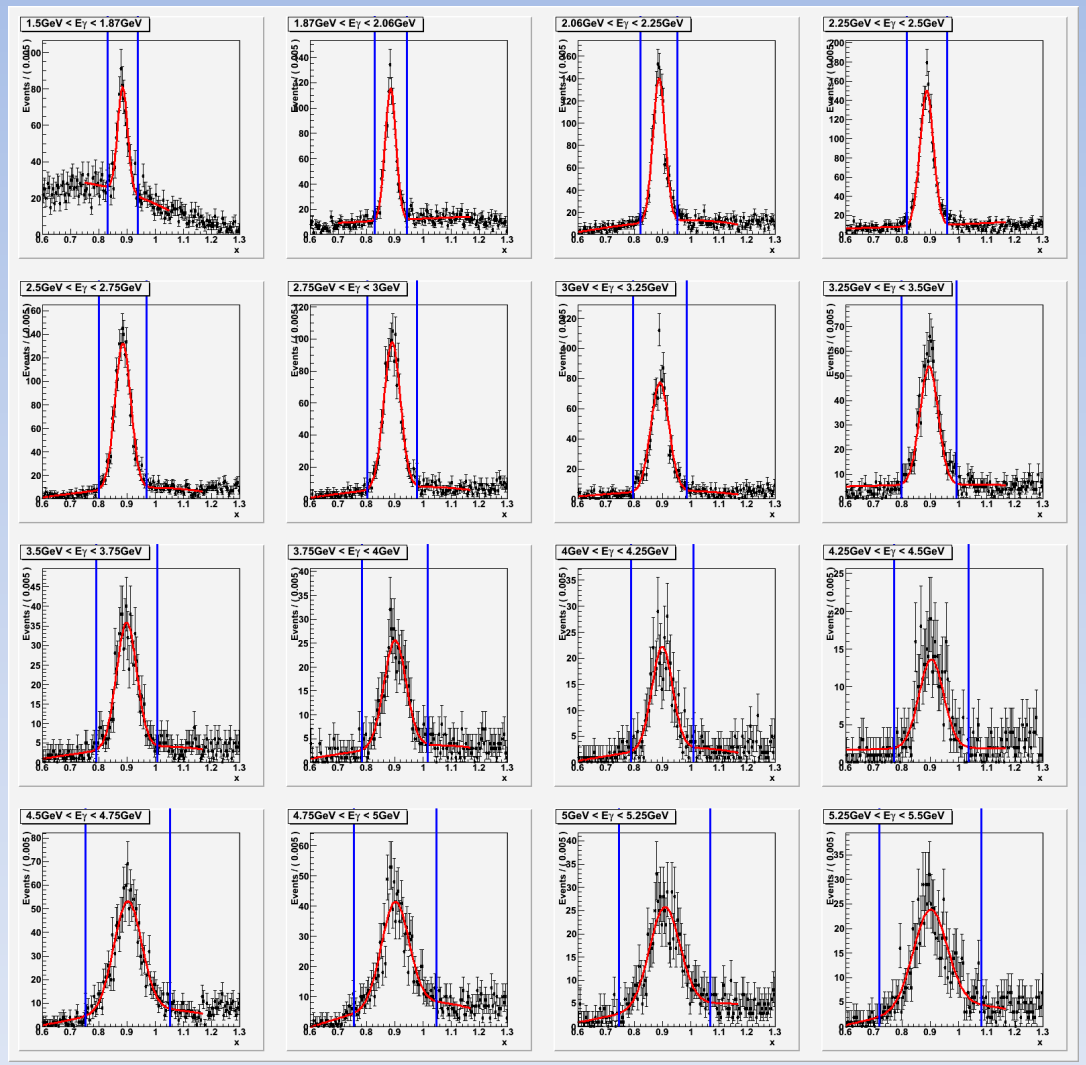

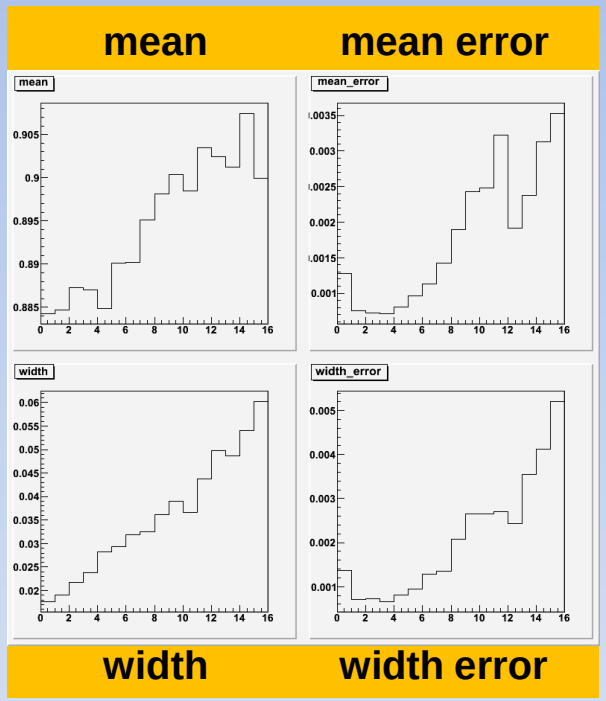

Proton

Missing Nucleon Mass

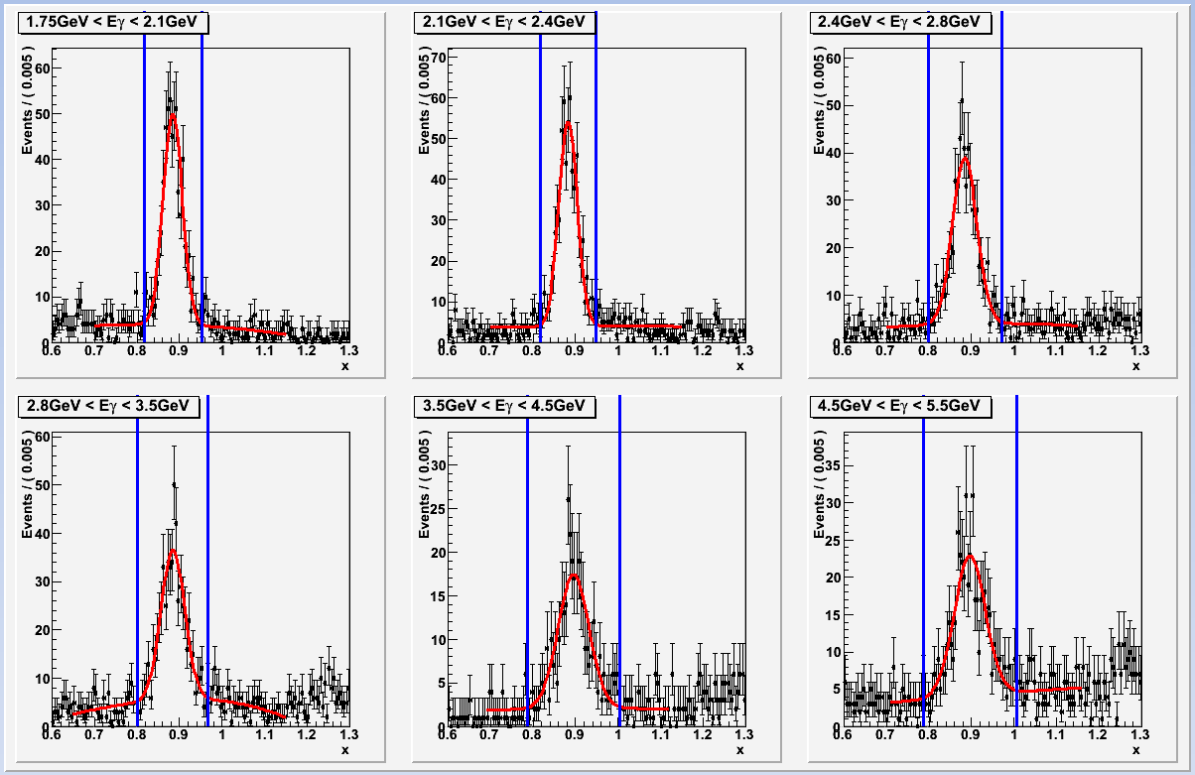

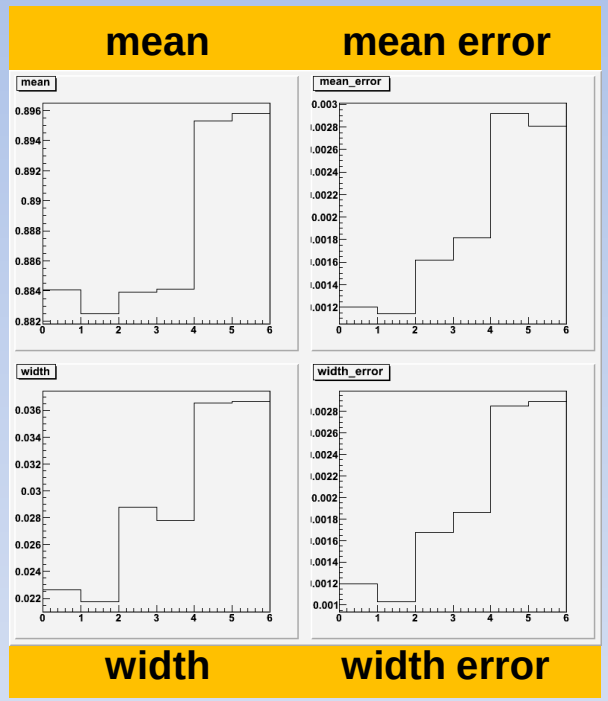

Missing Nucleon Momentum

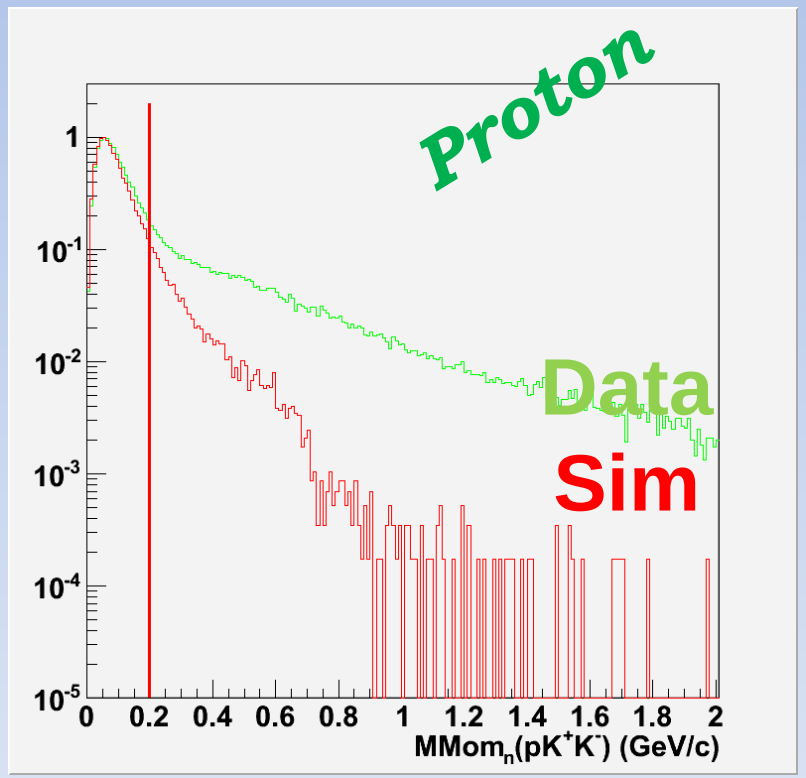

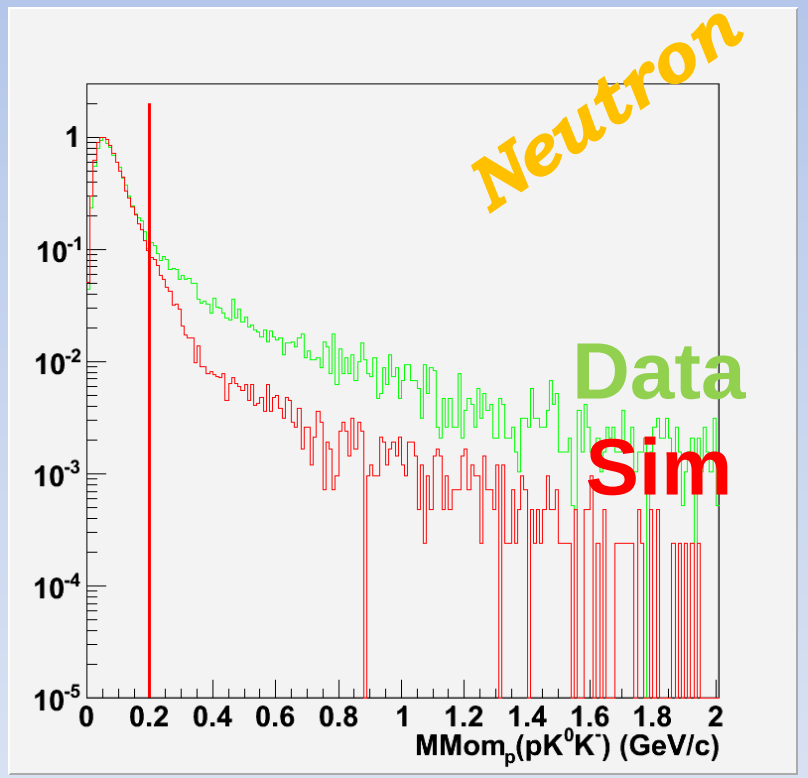

Proton

Kinematic Distribution

$1.5 < E_\gamma < 5.5$ GeV
16 bins, bin width 250 MeV

$-0.8 < \cos\theta_K^{-GJ} < 0.9$
6 bins, bin width varies

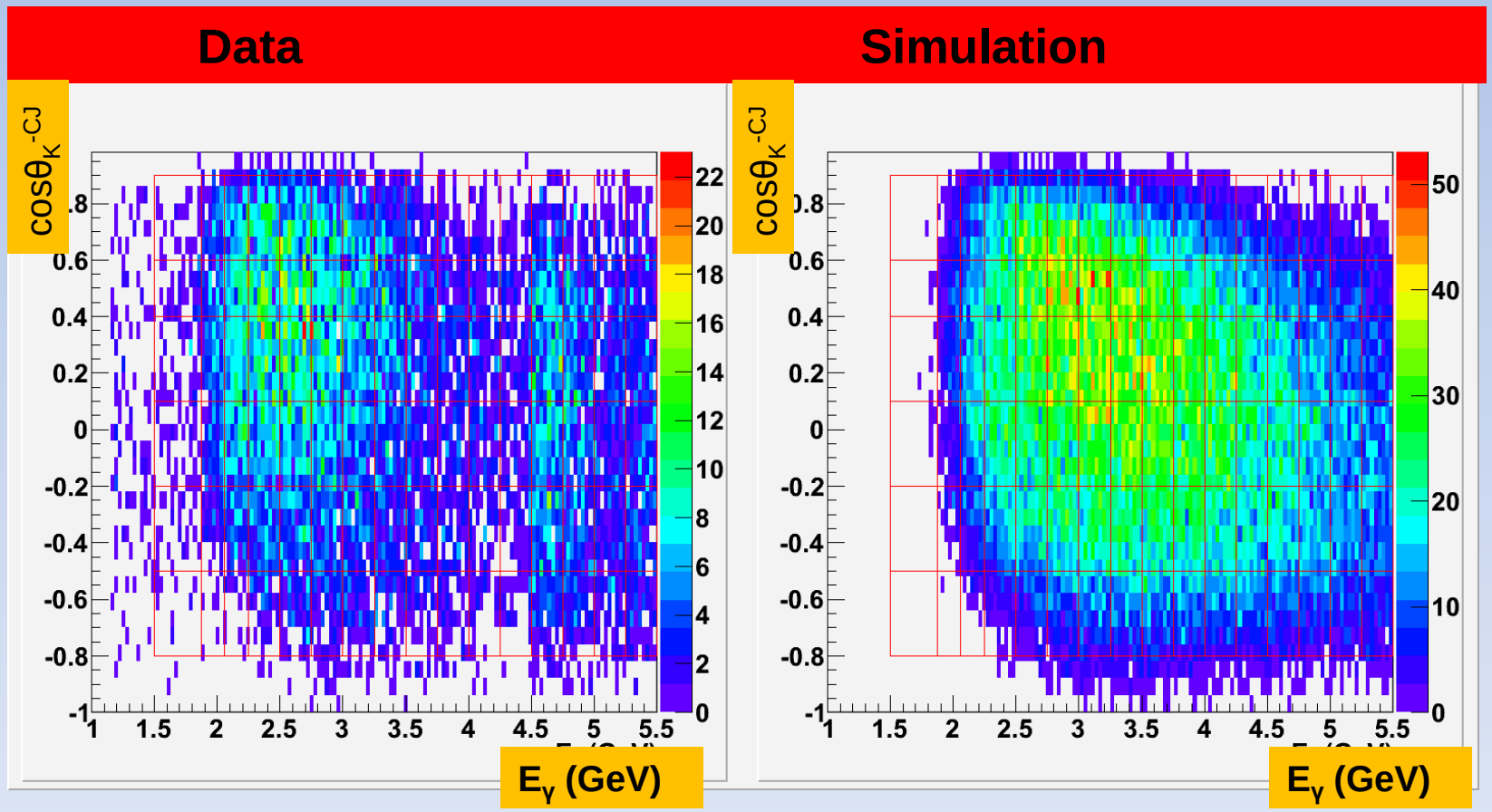

Neutron

Kinematic Distribution

$1.5 < E_\gamma < 5.5$ GeV
6 bins, bin width varies

$-0.8 < \cos\theta_K^{-GJ} < 0.9$
6 bins, bin width varies

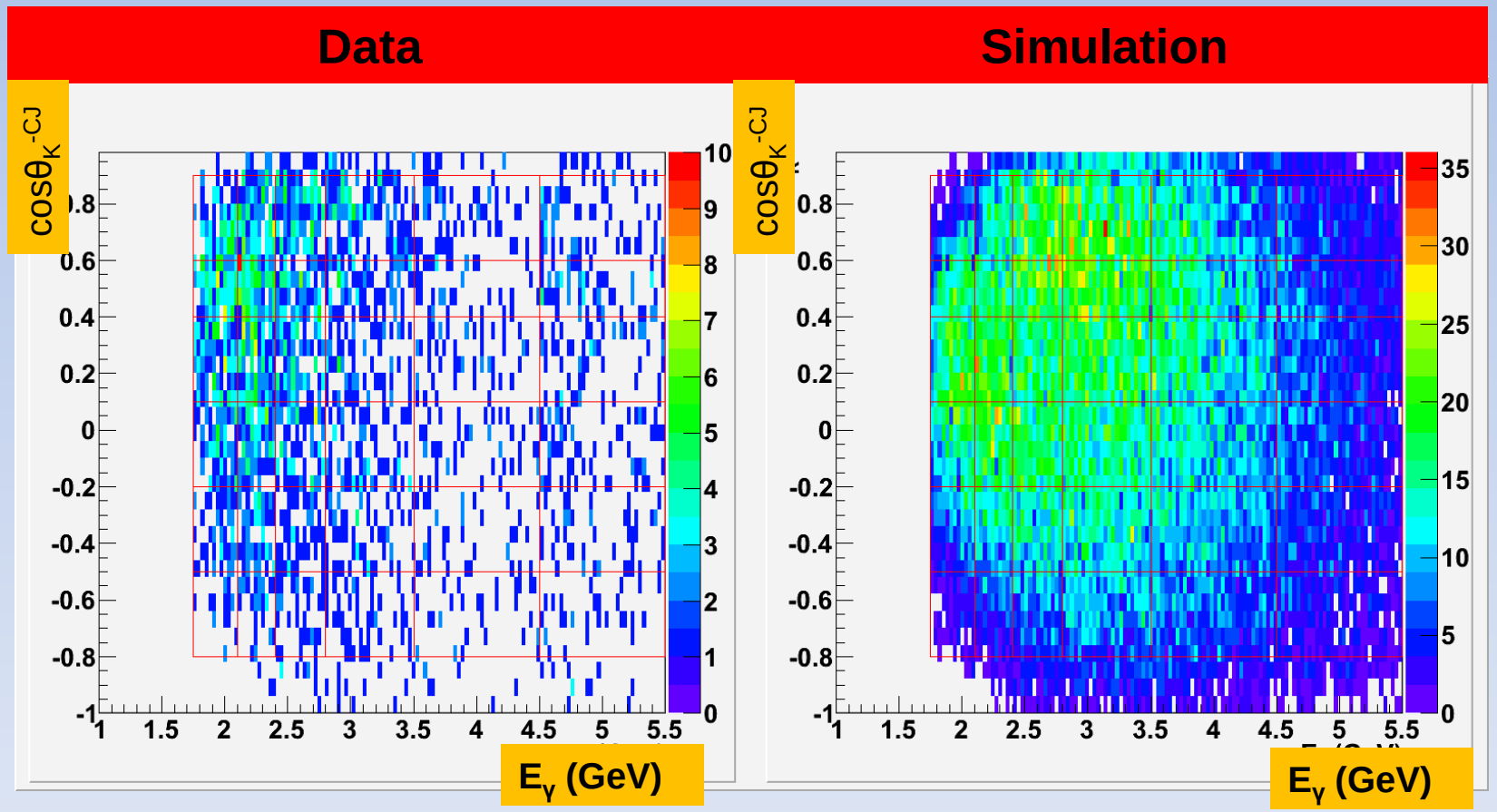

Proton

Yield Extraction (data)

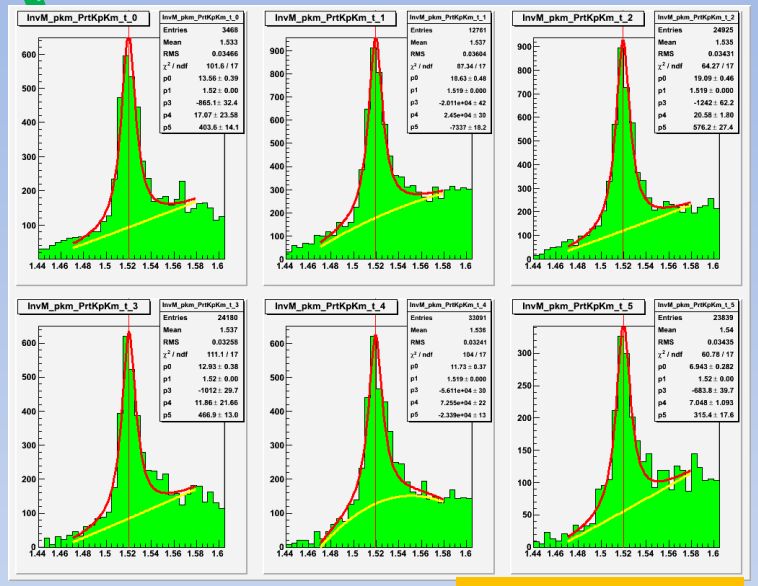

M(pK$^-$) (GeV)

$0.25 < t^* = -(t-t_0) < 3.0$ GeV^2
6 bins, bin width varies

$1.5 < E_\gamma < 5.5$ GeV
16 bins, bin width 250 MeV

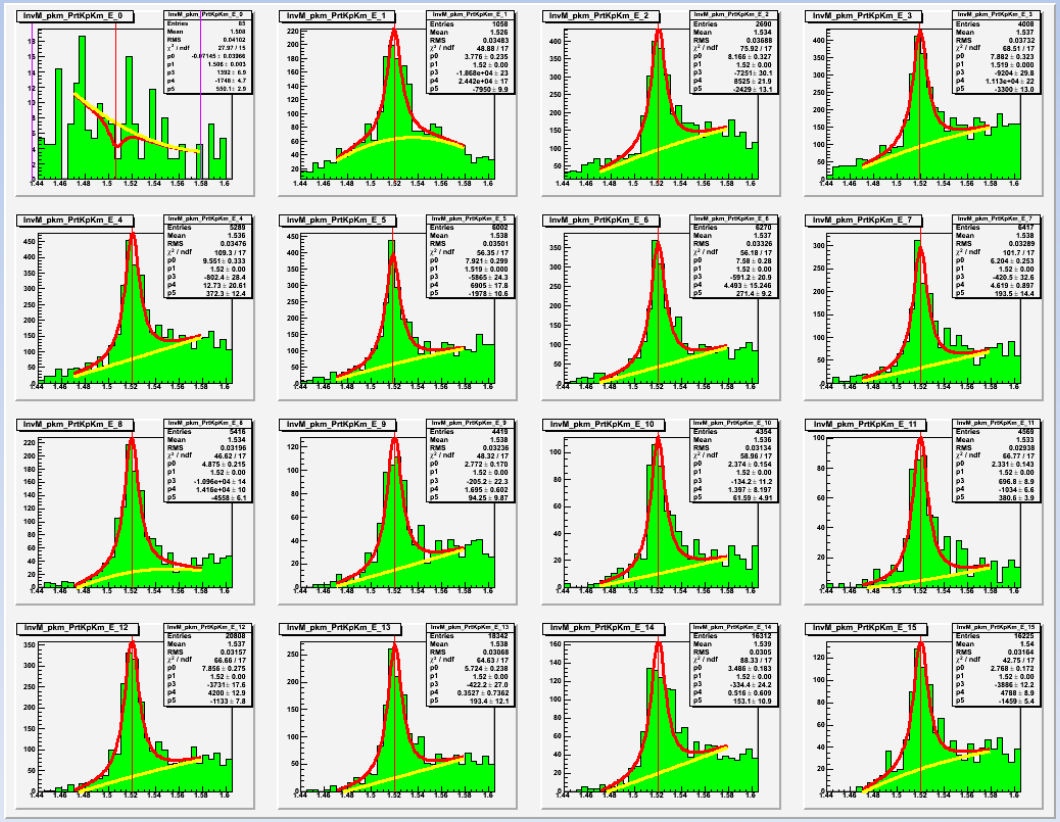

M(pK$^-$) (GeV)

Neutron

Yield Extraction (data)

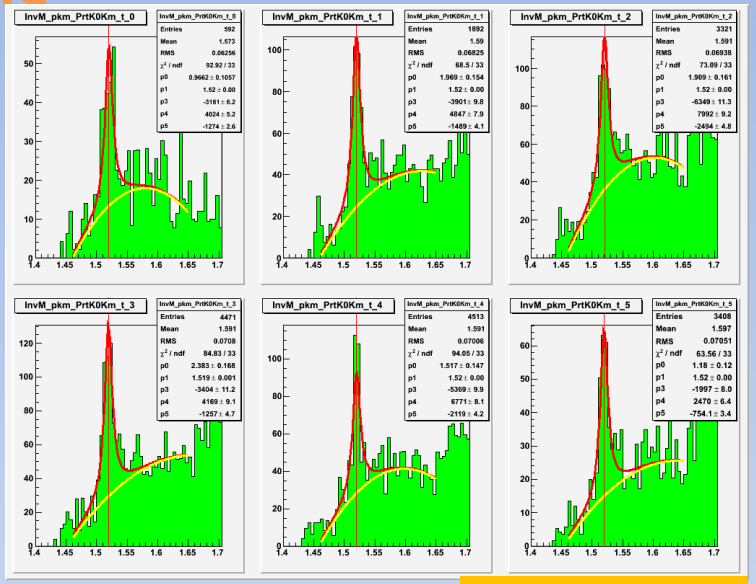

M(pK$^-$) (GeV)

$1.5 < E_\gamma < 5.5$ GeV
6 bins, bin width varies

$0.0 < t^* = -(t-t_0) < 3.0$ GeV^2
6 bins, bin width varies

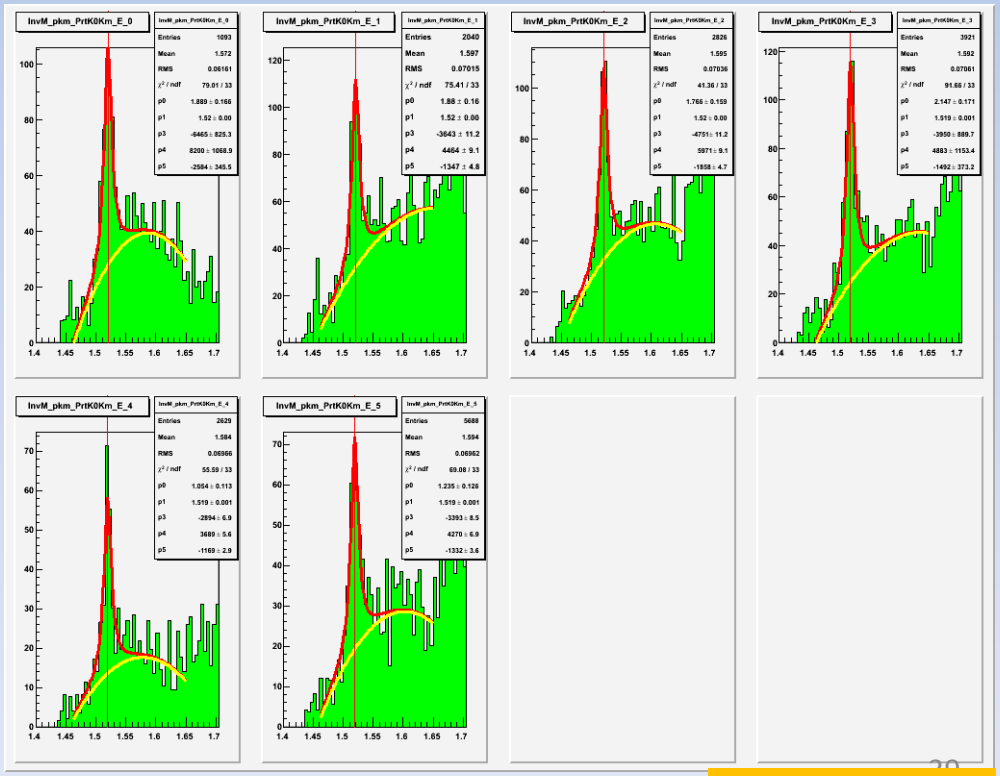

M(pK$^-$) (GeV)

Yield and Acceptance

Proton

	Data	Simulation		
	Yield	Yield	# of generated	Acceptance
Eγ bin	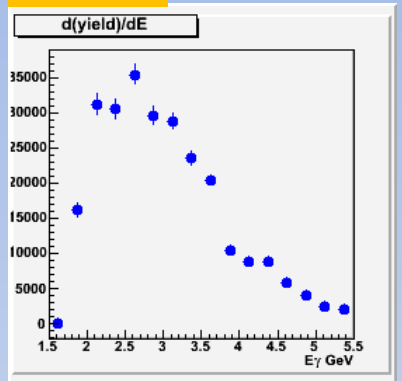	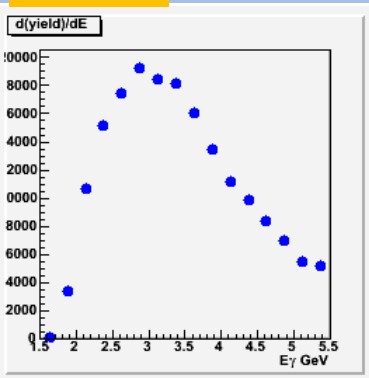	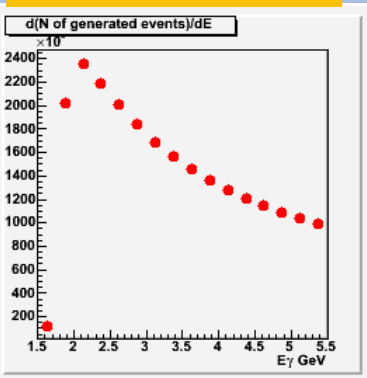	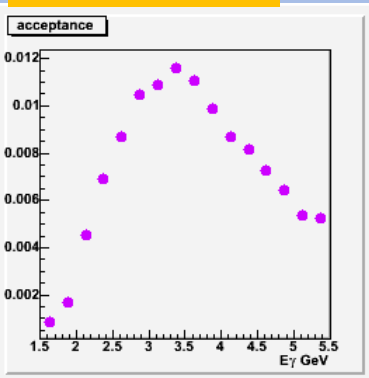
t* bin	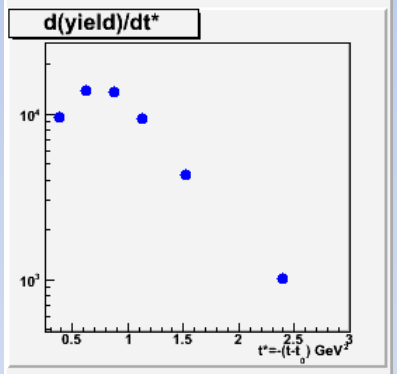	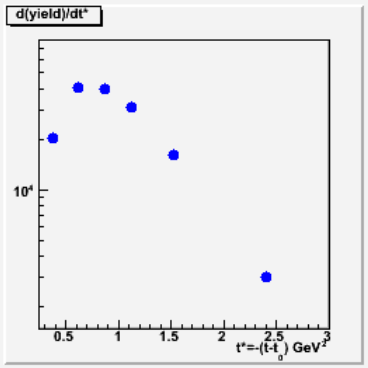	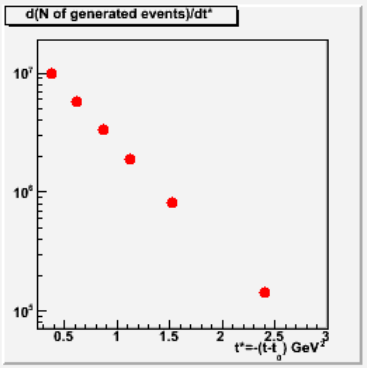	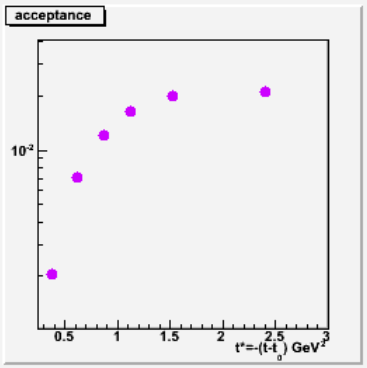
Eγ, t* bin	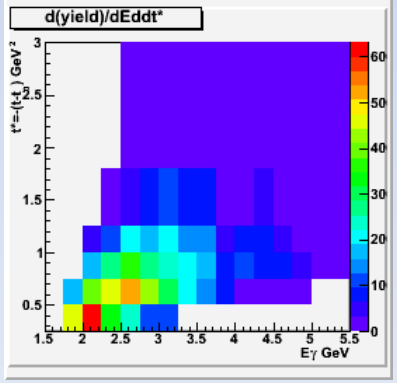	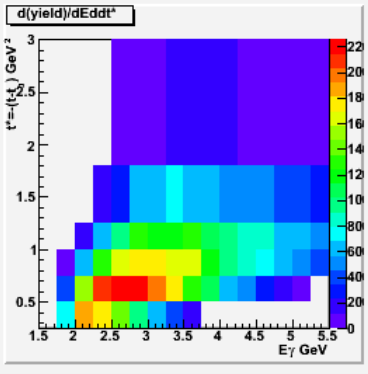	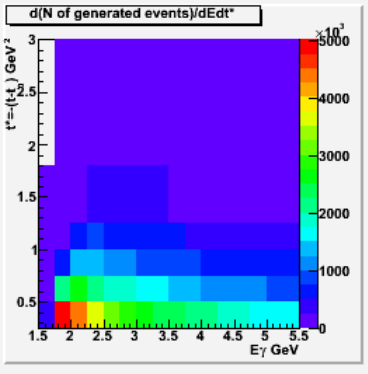	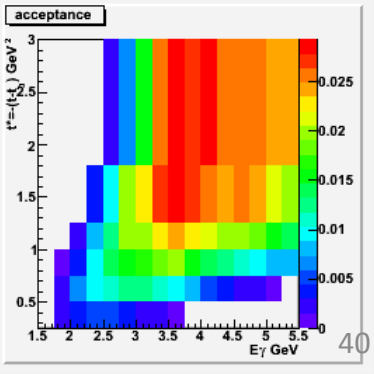

Yield and Acceptance

Neutron

	Data	Simulation		
	Yield	Yield	# of generated	Acceptance
Eγ bin	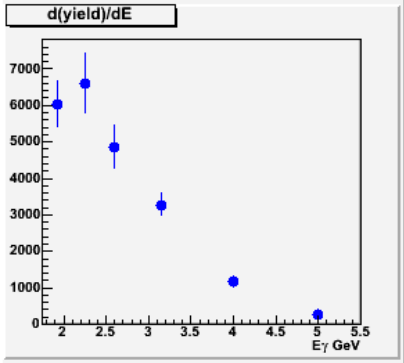	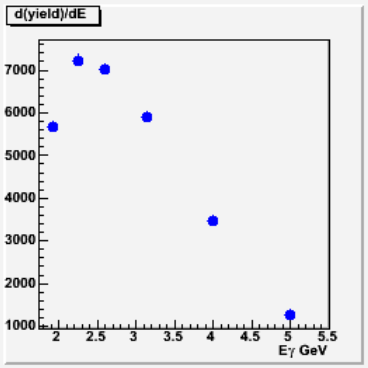	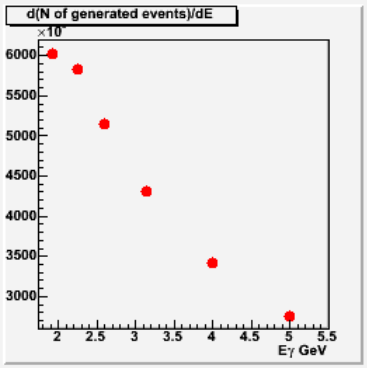	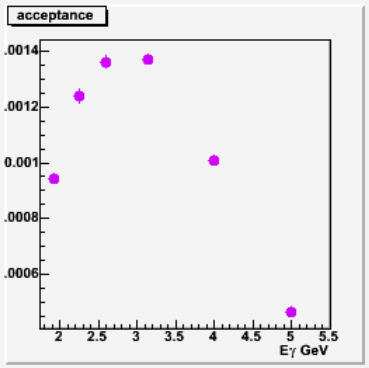
t* bin	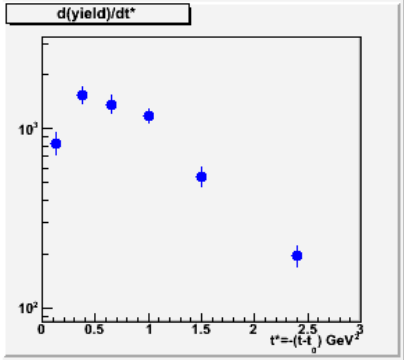	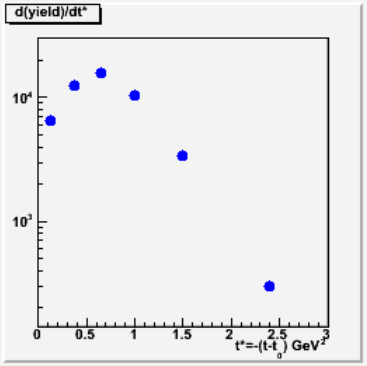	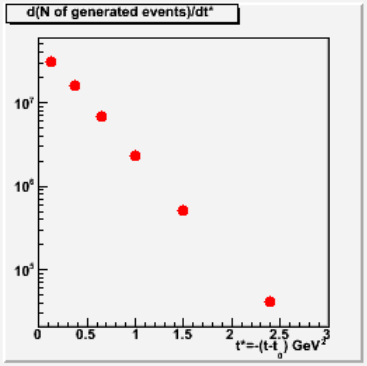	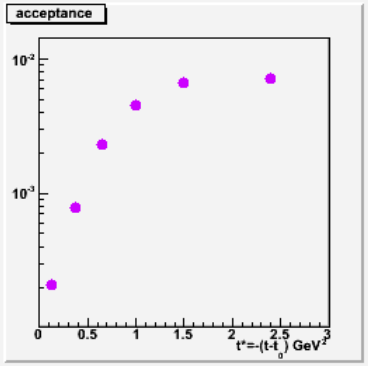
Eγ, t* bin	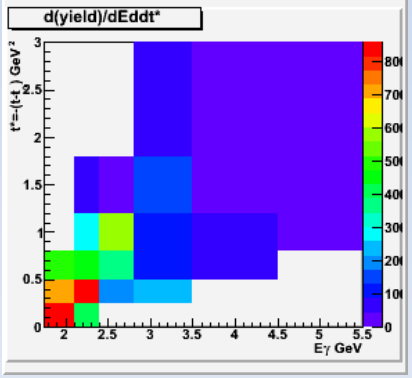	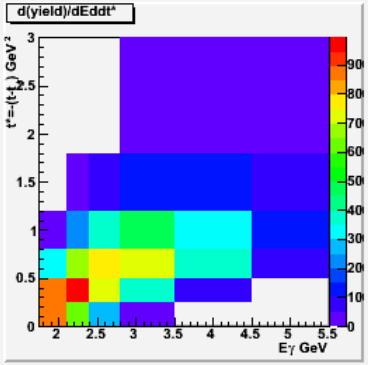	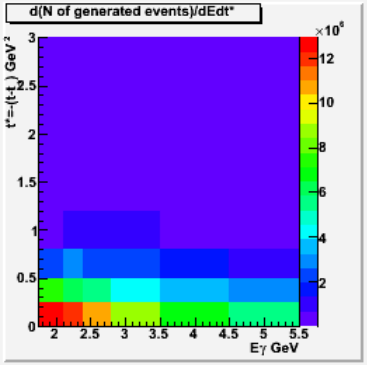	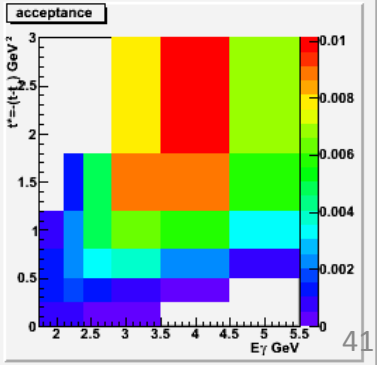

SAPHIR

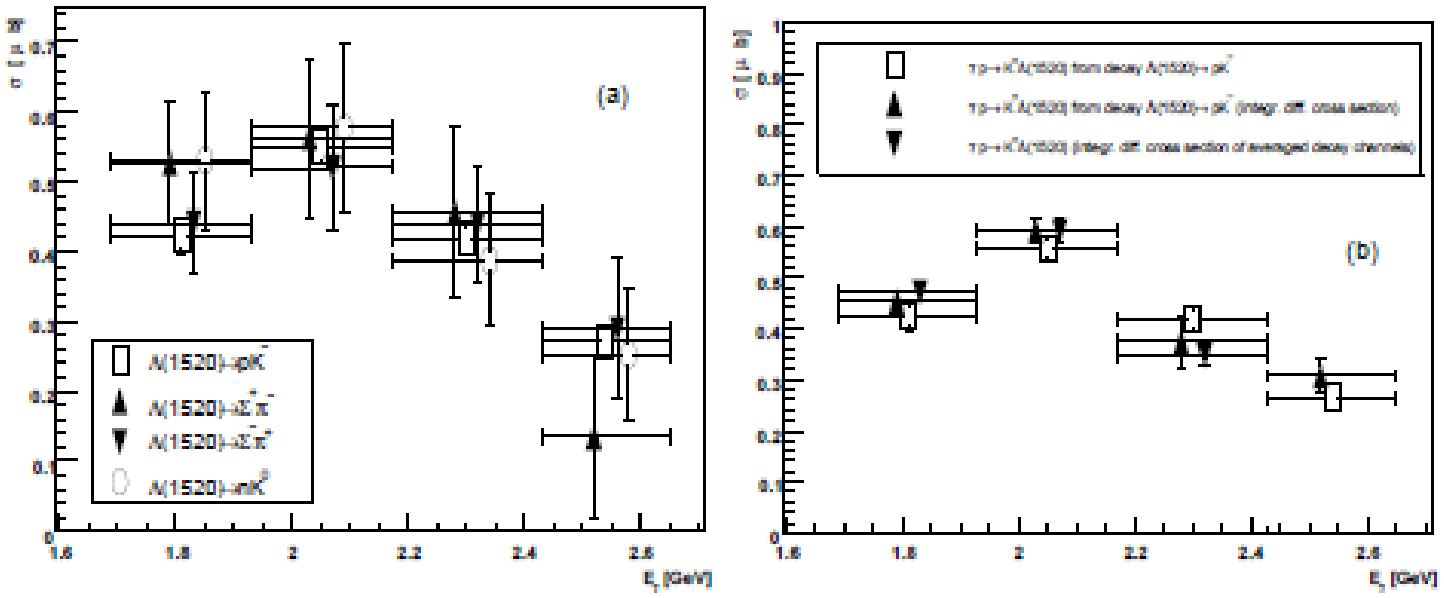

Fig. 13. (a) Total cross section for the reaction $\gamma p \to K^+ \Lambda(1520)$ as determined in different decay channels, (b) Comparison of the total cross sections for the dominant decay channel $\Lambda(1520) \to pK^-$ (see (a), squares) gained via integration of the differential cross sections $d\sigma/dt$ (upward triangles), and the averaged and integrated differential cross sections (downward triangles) from the four decay channels presented in (a).

SAPHIR

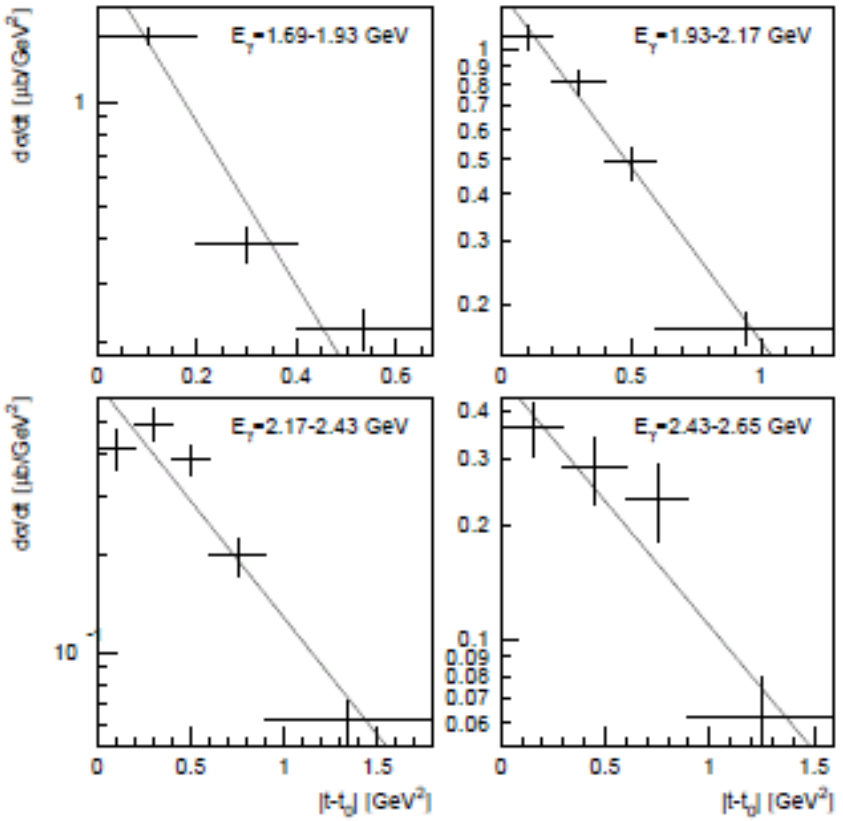

Fig. 14. Differential cross section for the reaction $\gamma p \to K^+\Lambda(1520)$ determined via the decay channel $\Lambda(1520) \to pK^-$ in four photon energy bins as a function of $|t - t_0|$; t_0 denotes the minimal kinematically allowed squared four-momentum transfer, which was calculated on an event-by-event basis.